

Supplementary Information

For

Supramolecular electrochemical probe based on the system of tetrazole derivative pillar[5]arene/methylene blue

Lyaysan I. Makhmutova,^a Dmitriy N. Shurpik,^{a*} Olga A. Mostovaya,^a Natalia R. Lachugina,^a
Alexander V. Gerasimov,^a Adelya Guseinova,^a Gennady A. Evtugyn,^a Ivan I. Stoikov^{a*}

^a *A.M. Butlerov Chemical Institute, Kazan Federal University, Kremlevskaya, 18, 420008 Kazan, Russia*

Table of contents

1. NMR, MALDI TOF MS, IR spectra of the compounds 2, 3, 4, 6, 7, 8.....	2
2. Thermal Gravimetric Analysis of 3, 4 and 7, 8.....	14
3. UV spectra and Bindfit (Fit data to 1:1, 1:2 and 2:1 Host-Guest equilibria).....	16
4. Dynamic light scattering.....	22
6. Electrochemistry.....	24
7. Transmission electron microscopy.....	26

1. NMR, MALDI TOF MS, IR spectra of the compounds 2, 3, 4, 6, 7, 8

Figure S01. ^1H NMR spectrum of 1,4-bis(2-thiocyanoethoxy)benzene (**2**), DMSO- d_6 , 298 K, 400 MHz.

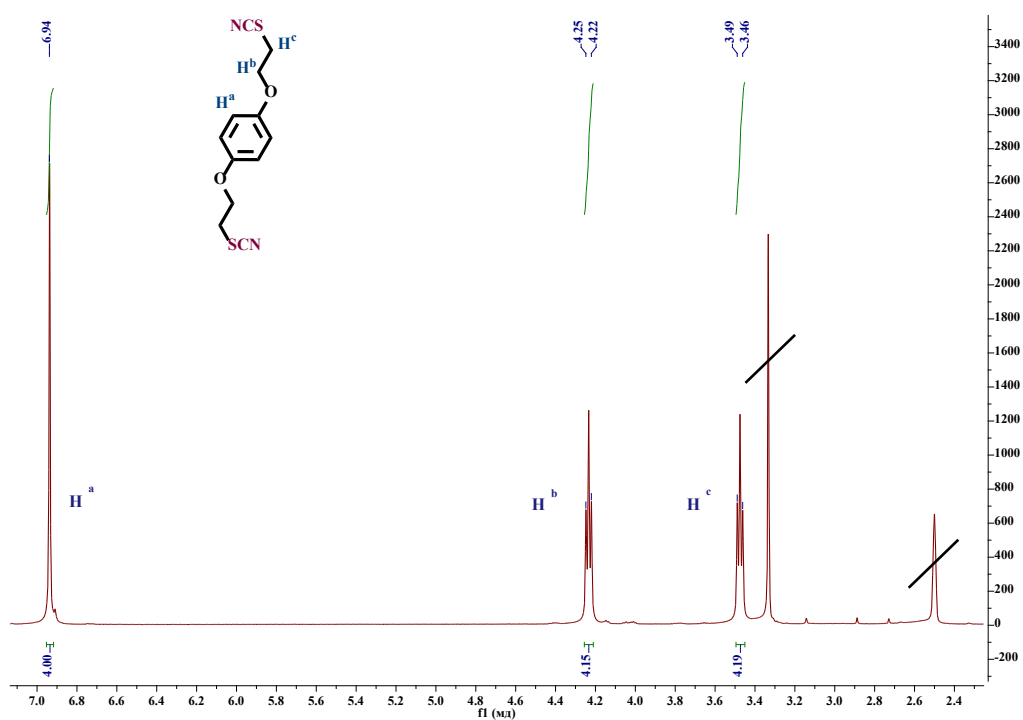


Figure S02. ^{13}C NMR spectrum of 1,4-bis(2-thiocyanoethoxy)benzene (**2**), DMSO- d_6 , 298 K, 100 MHz.

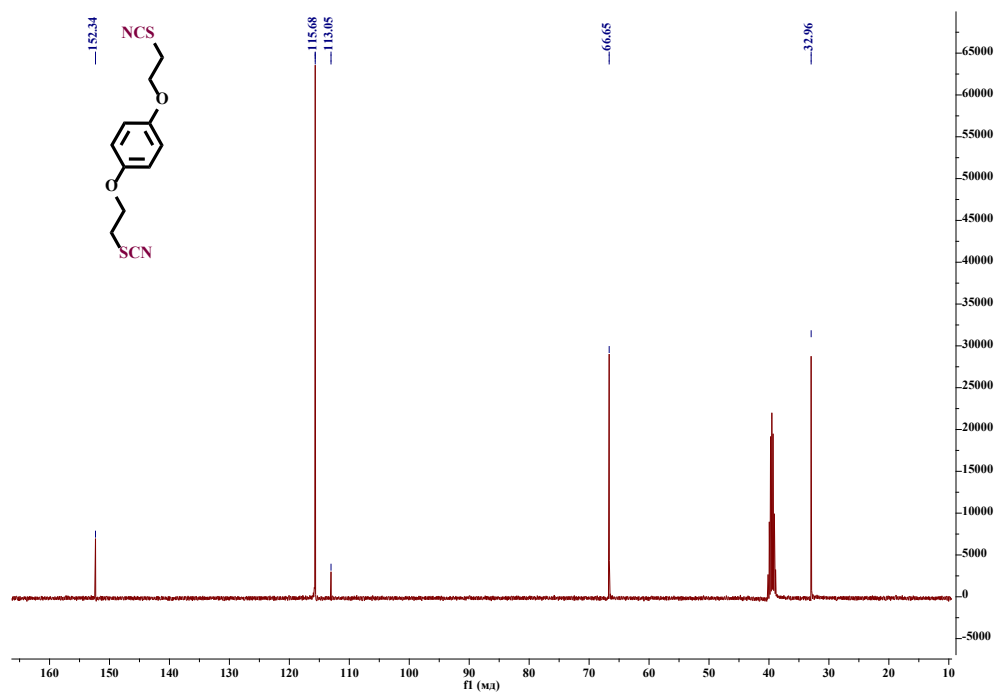


Figure S03. Mass spectrum (GC MS) of 1,4-bis(2-thiocyanoethoxy)benzene (2).

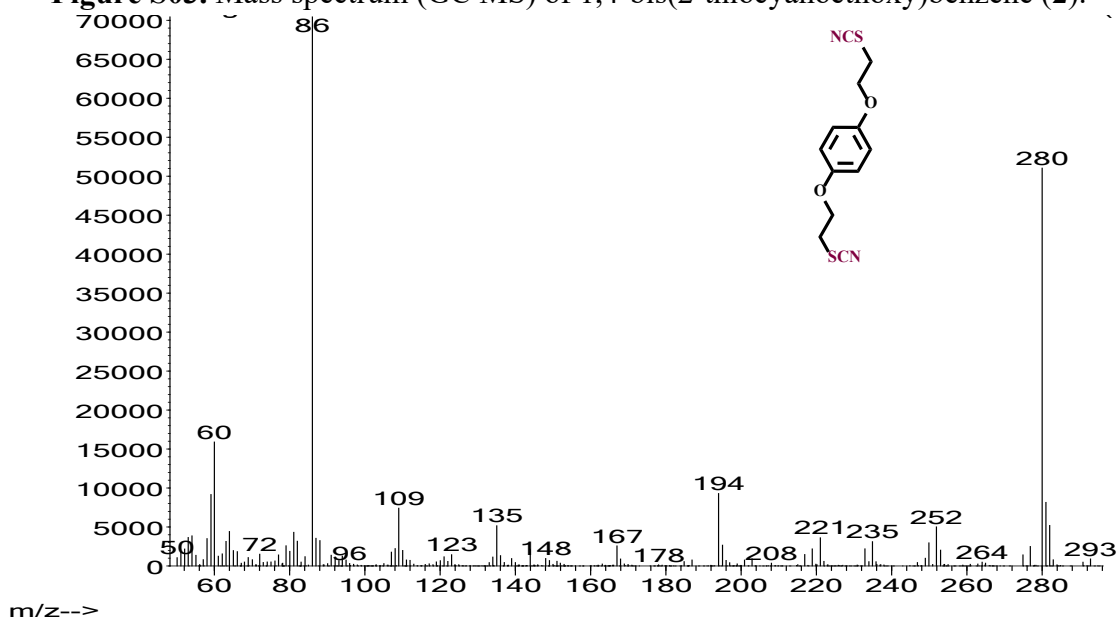


Figure S04. IR spectrum of 1,4-bis(2-thiocyanoethoxy)benzene (2).

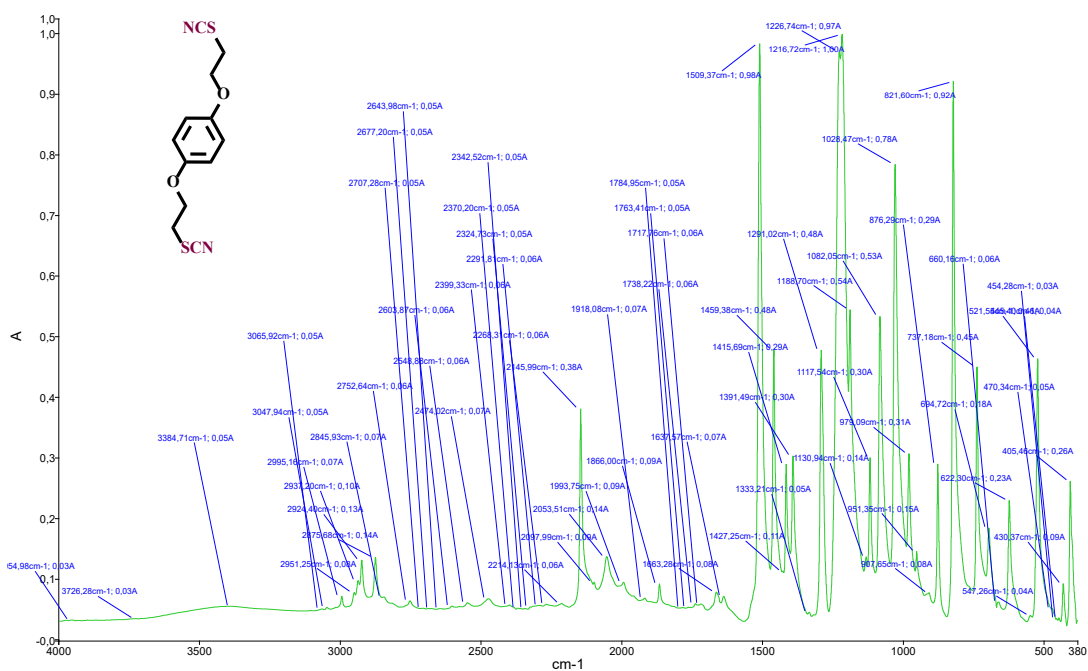


Figure S05. ^1H NMR spectrum of 4, 8, 14, 18, 23, 26, 28, 31, 32, 35-deca(2-thiocyanoethoxy)pillar[5]arene (**6**), DMSO- d_6 , 298 K, 400 MHz

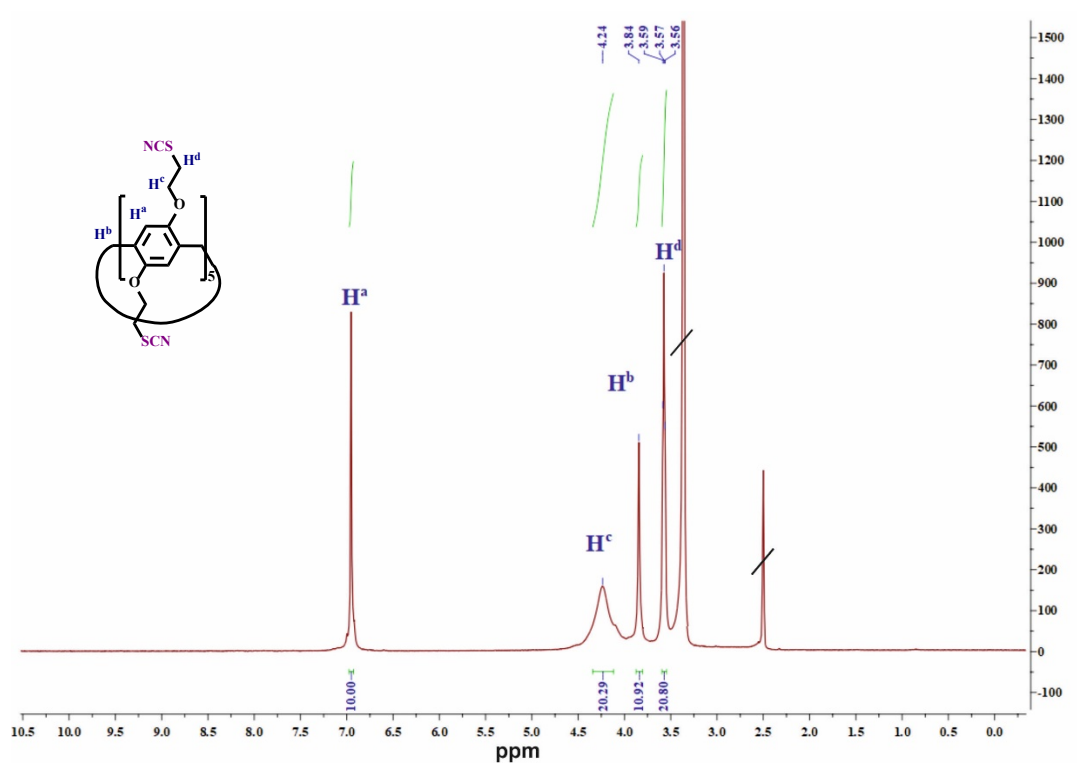


Figure S06. ^{13}C NMR spectrum of 4, 8, 14, 18, 23, 26, 28, 31, 32, 35-deca(2-thiocyanoethoxy)pillar[5]arene (**6**), DMSO- d_6 , 298 K, 100 MHz.

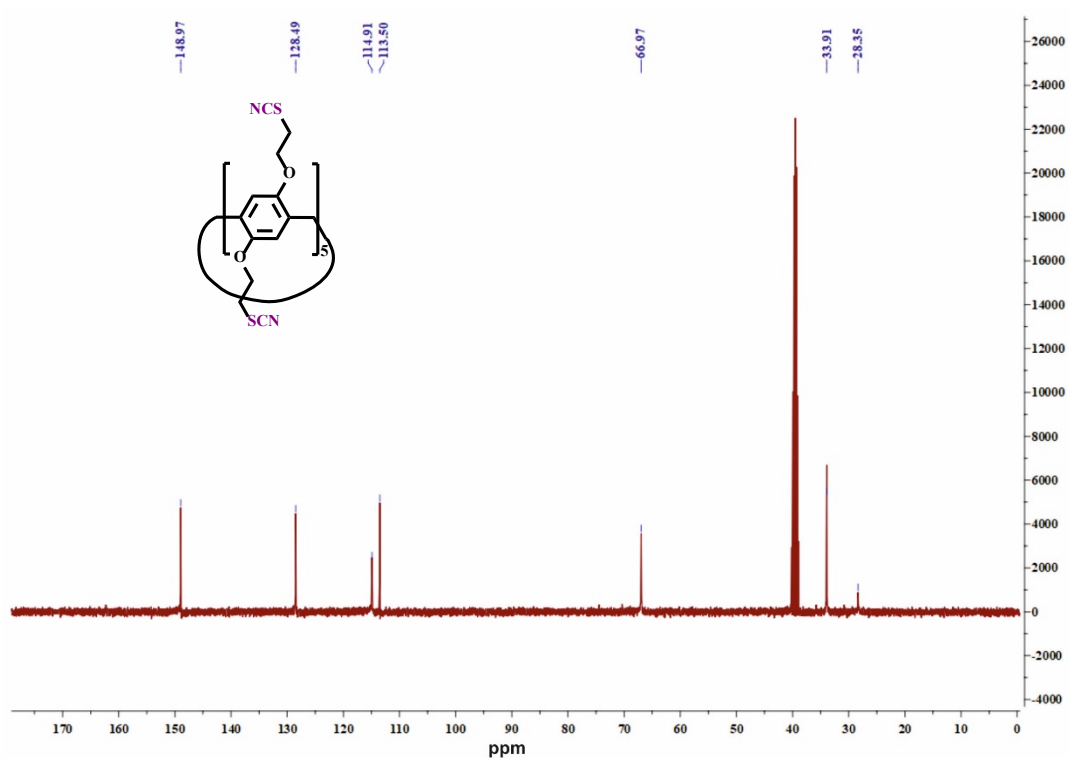


Figure S07. IR spectrum of 4, 8, 14, 18, 23, 26, 28, 31, 32, 35-deca(2-thiocyanoethoxy)pillar[5]arene (**6**).

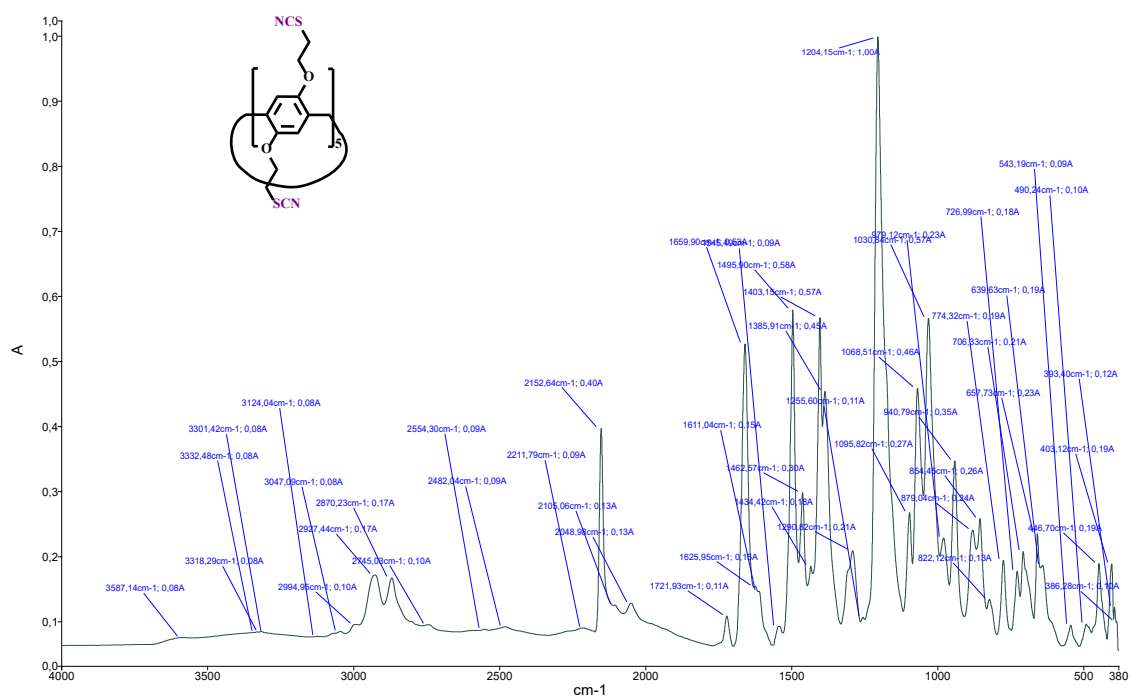


Figure S08. Mass spectrum (MALDI-TOF, 4-nitroaniline matrix) of 4, 8, 14, 18, 23, 26, 28, 31, 32, 35-deca(2-thiocyanoethoxy)pillar[5]arene (**6**).

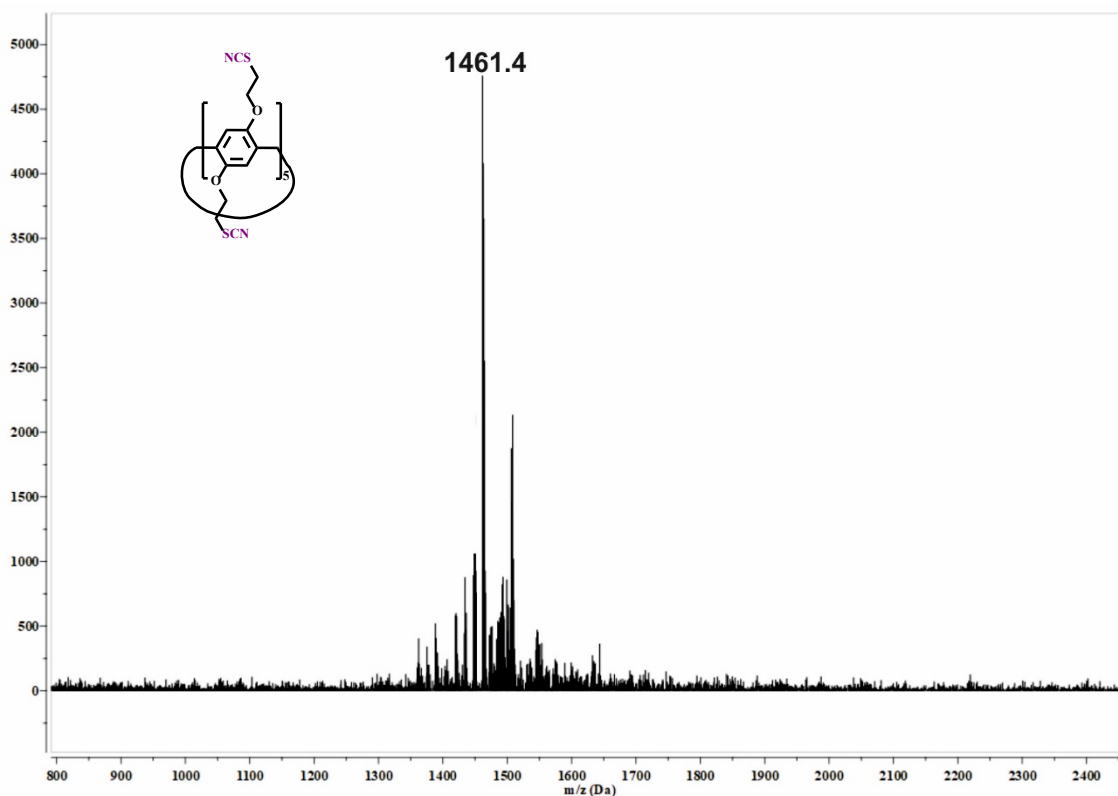


Figure S09. ^1H NMR spectrum of 1,4-bis(2-((1H-tetrazol-5-yl)thio)ethoxy)benzene (**3**), DMSO-d_6 , 298 K, 400 MHz

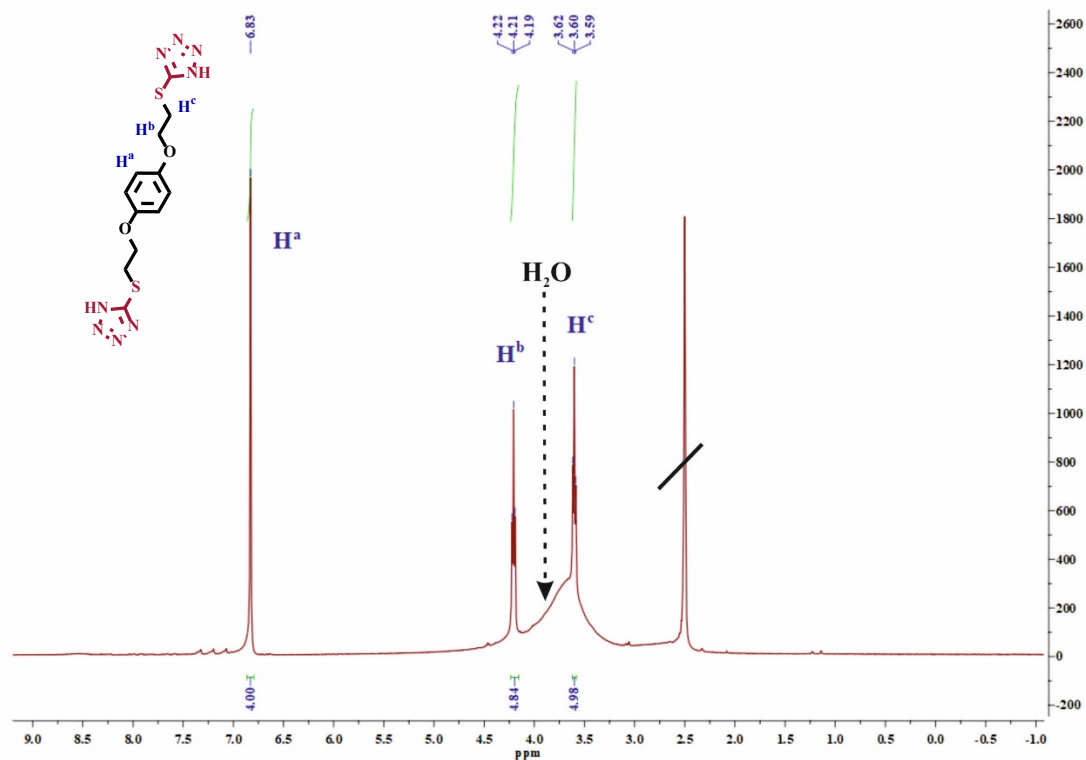


Figure S10. ^{13}C NMR spectrum of 1,4-bis(2-((1H-tetrazol-5-yl)thio)ethoxy)benzene (**3**), DMSO-d_6 , 298 K, 100 MHz.

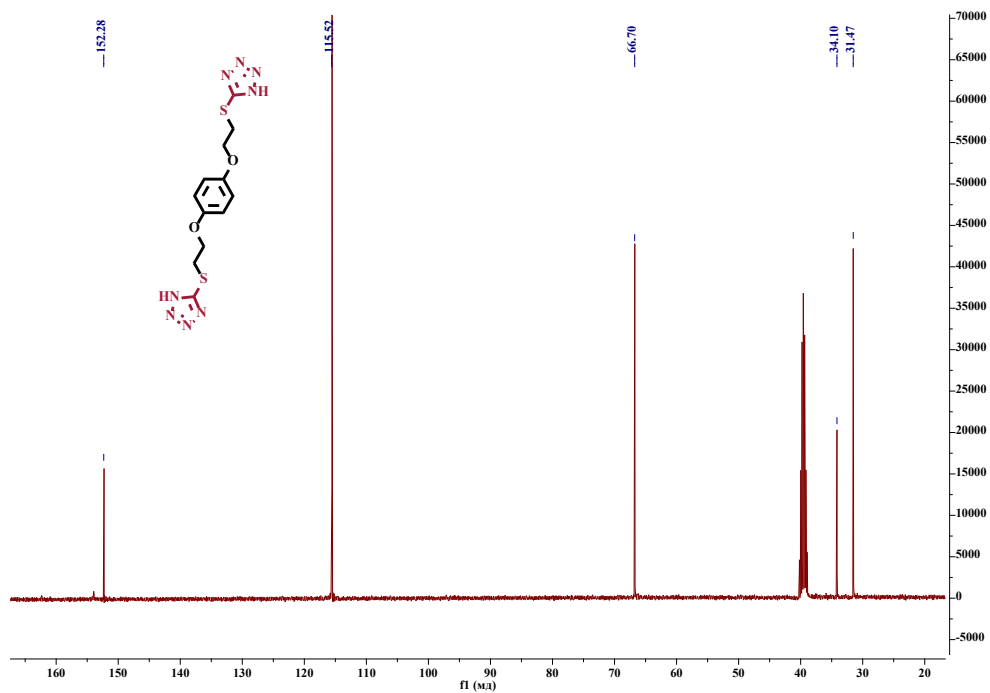


Figure S11. Mass spectrum (MALDI-TOF, 4-nitroaniline matrix) of 1,4-bis(2-((1H-tetrazol-5-yl)thio)ethoxy)benzene (**3**)

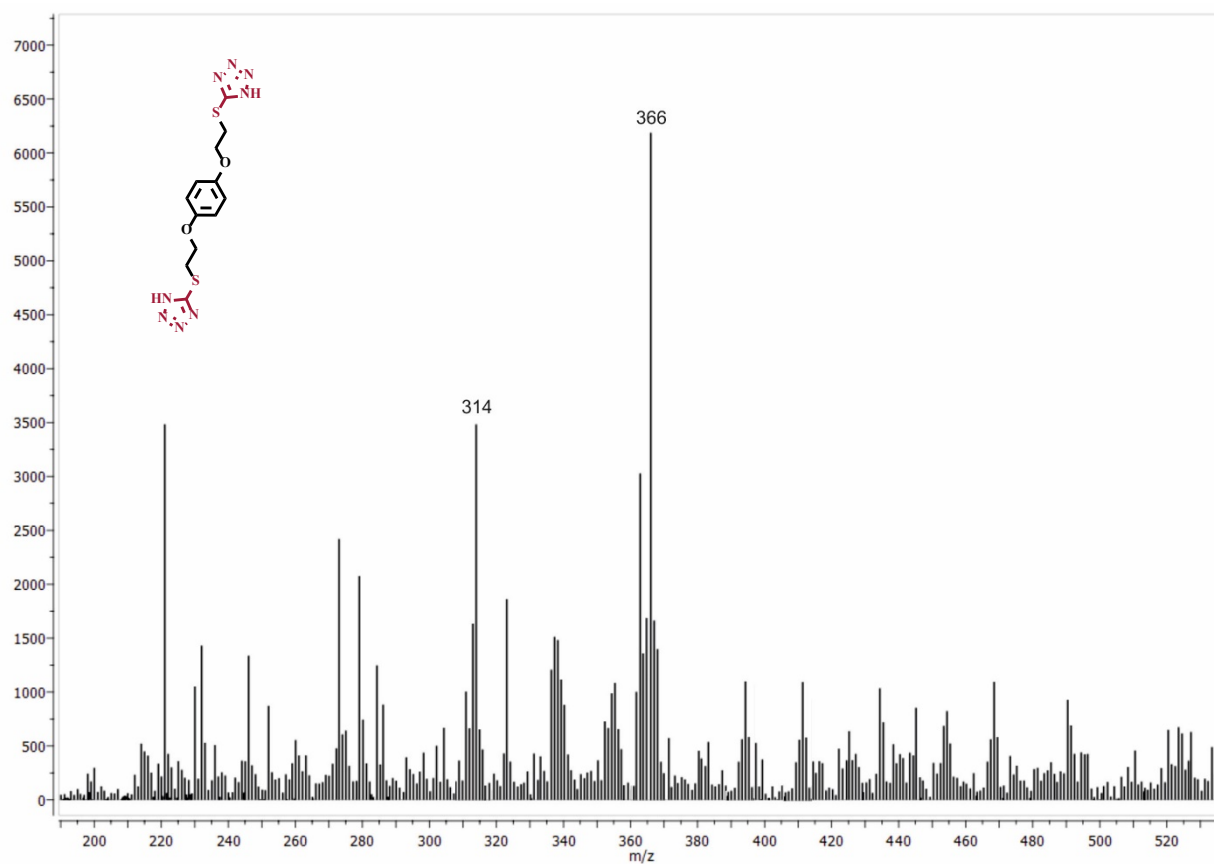


Figure S12. IR spectrum of 1,4-bis(2-((1H-tetrazol-5-yl)thio)ethoxy)benzene (**3**)

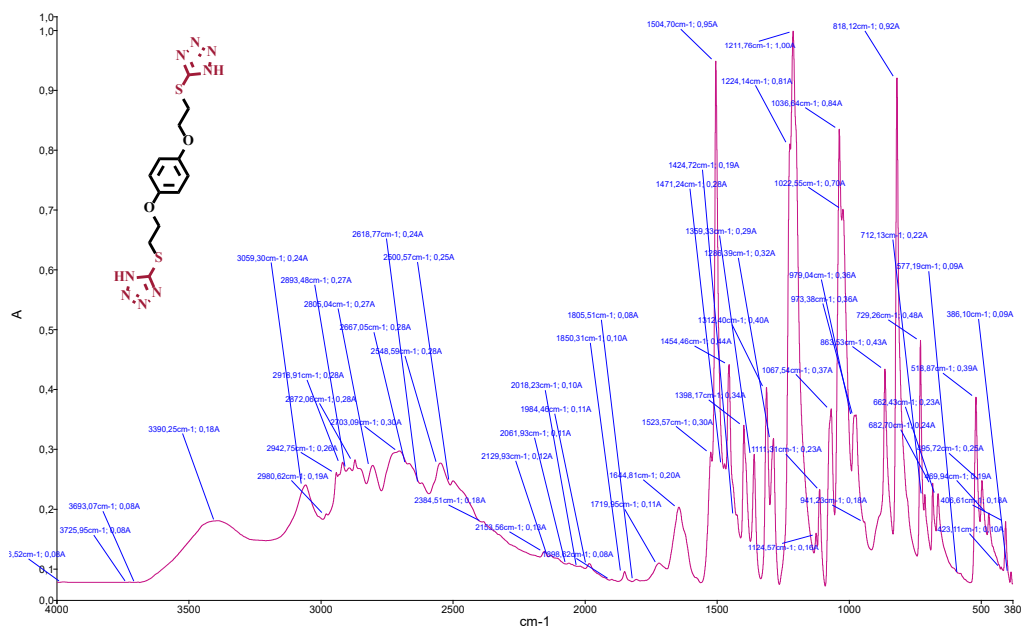


Figure S13. ^1H NMR spectrum of 4, 8, 14, 18, 23, 26, 28, 31, 32, 35-deca(2-((1H-tetrazol-5-yl)thio)ethoxy)pillar[5]arene (**7**), DMSO- d_6 , 298 K, 400 MHz.

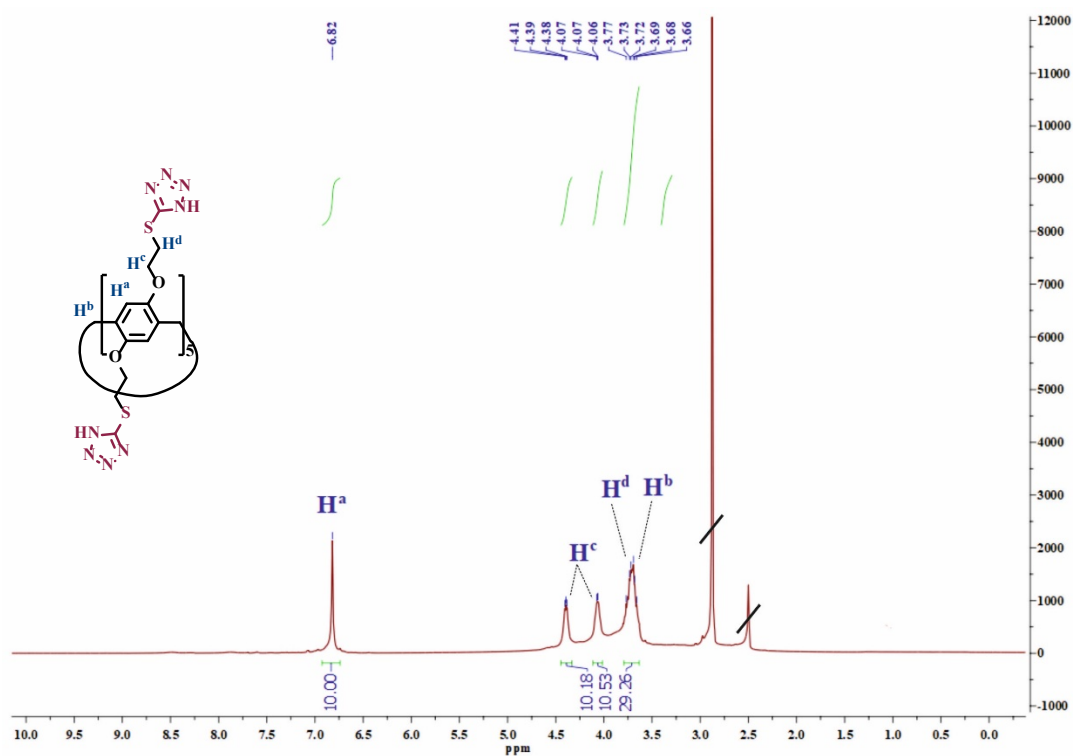


Figure S14. ^{13}C NMR spectrum of 4, 8, 14, 18, 23, 26, 28, 31, 32, 35-deca(2-((1H-tetrazol-5-yl)thio)ethoxy)pillar[5]arene (**7**), DMSO- d_6 , 298 K, 100 MHz.

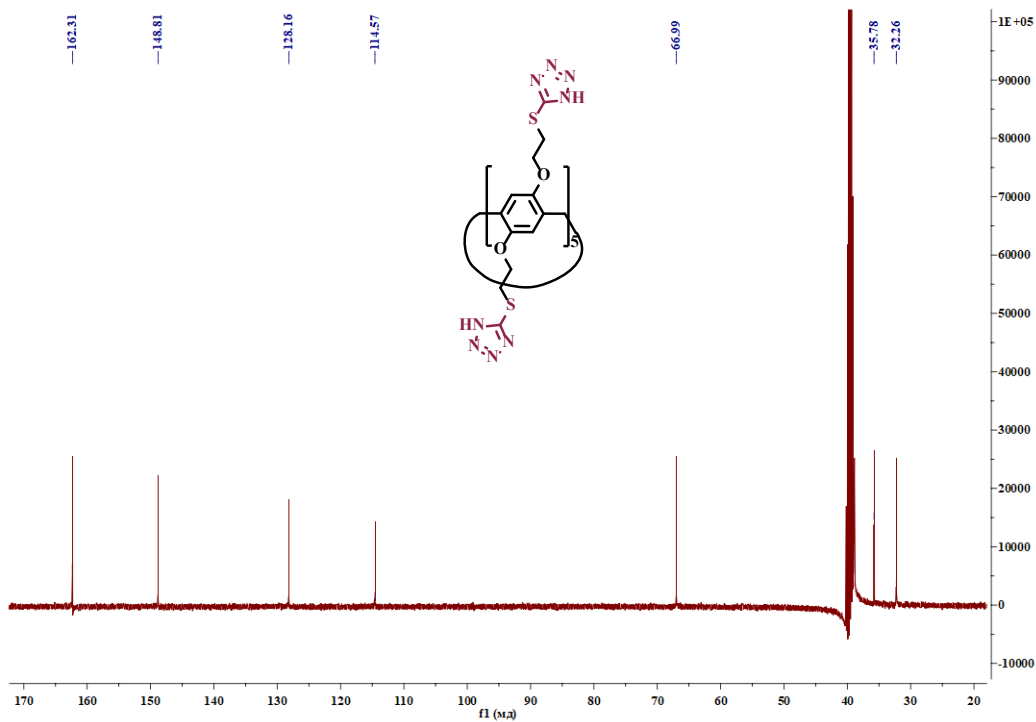


Figure S15. Mass spectrum (MALDI-TOF, 4-nitroaniline matrix) of 4, 8, 14, 18, 23, 26, 28, 31, 32, 35-deca(2-((1H-tetrazol-5-yl)thio)ethoxy)pillar[5]arene (**7**).

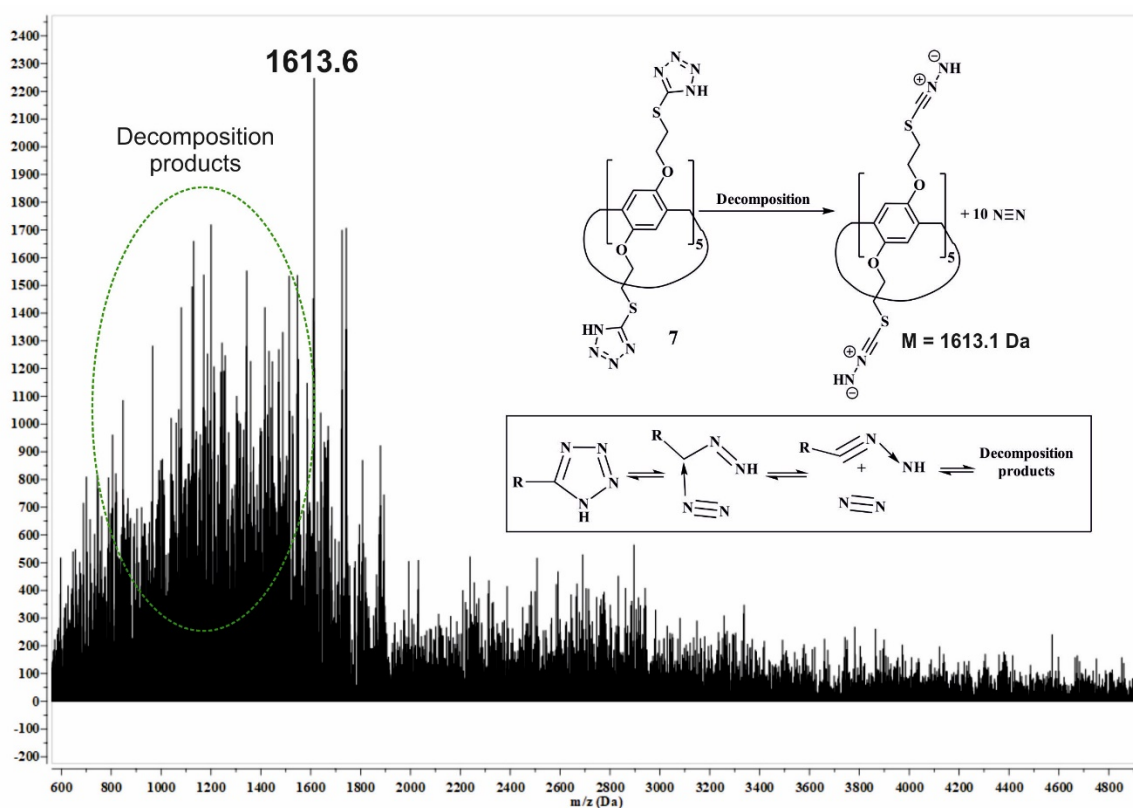


Figure S16. IR spectrum of 4, 8, 14, 18, 23, 26, 28, 31, 32, 35-deca(2-((1H-tetrazol-5-yl)thio)ethoxy)pillar[5]arene (**7**).

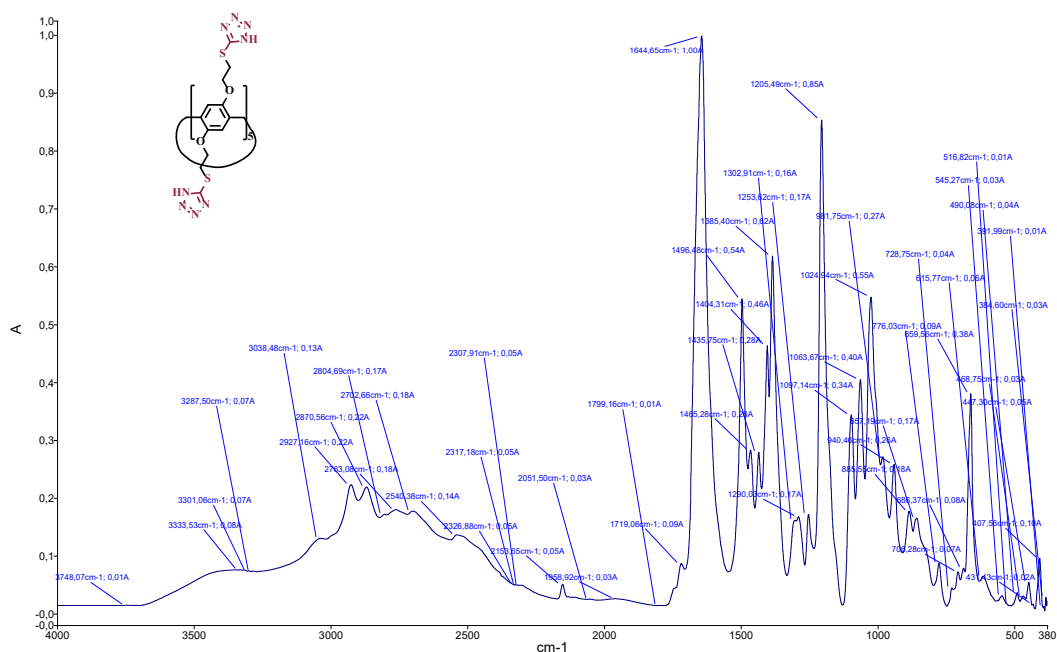


Figure S17. ^1H NMR spectrum of Ammonium salt of compound **4**, D_2O , 298 K, 400 MHz.

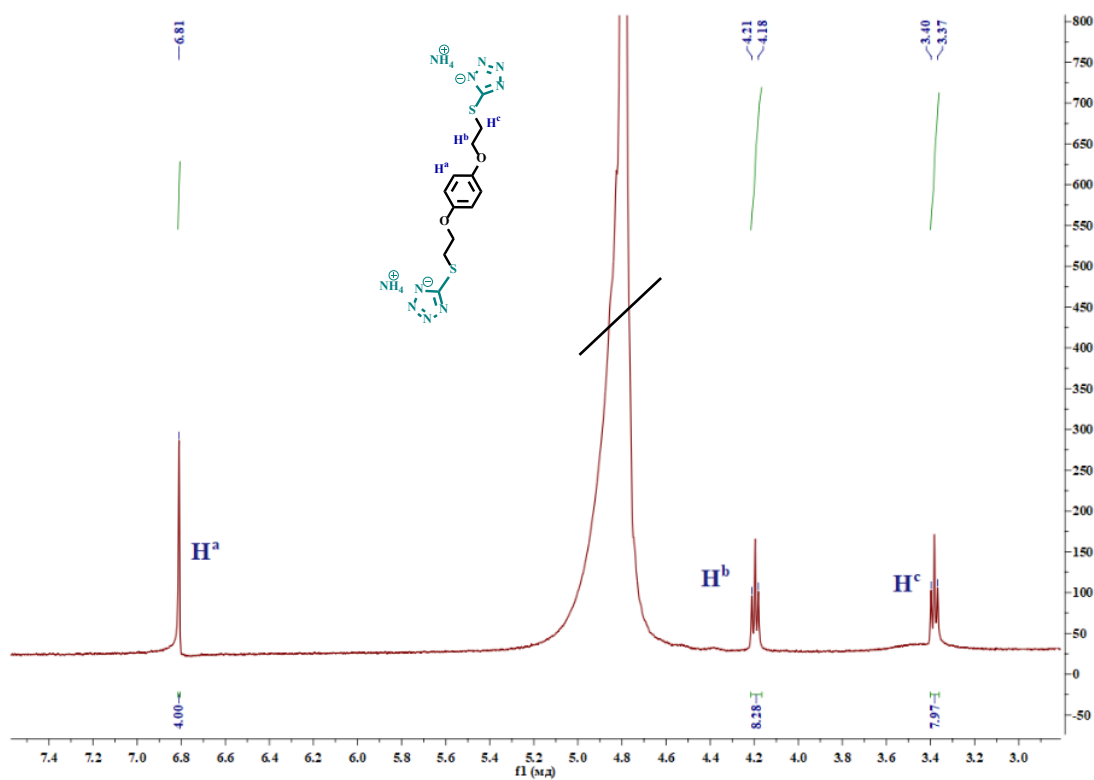


Figure S18. ^{13}C NMR spectrum of Ammonium salt of compound (**4**), D_2O , 298 K, 100 MHz

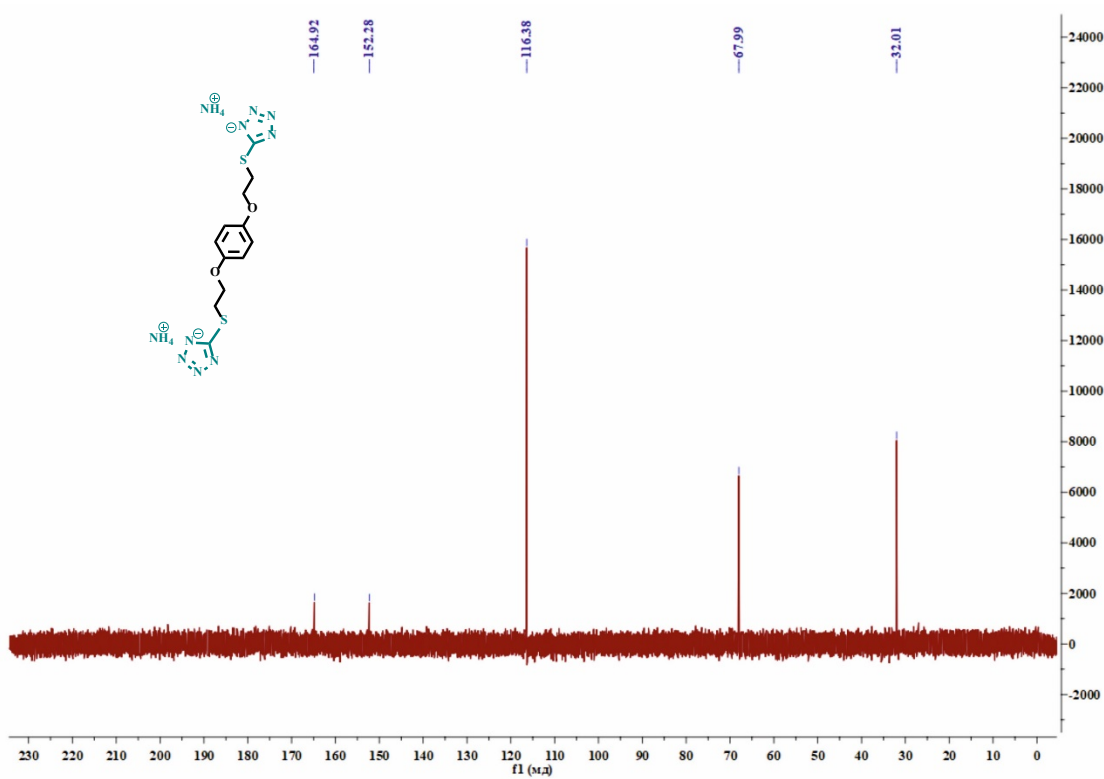


Figure S19. Mass spectrum (ESI) of Ammonium salt of compound (4).

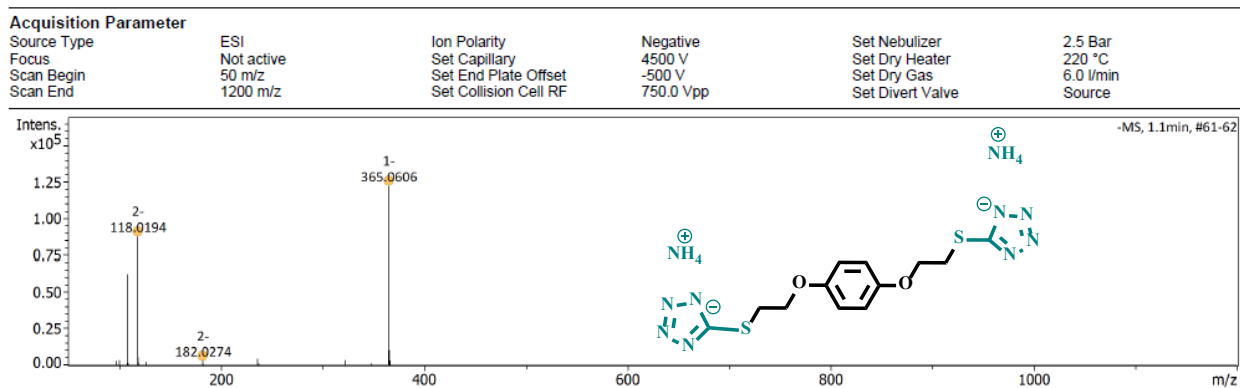


Figure S20. IR spectrum of Ammonium salt of compound (4).

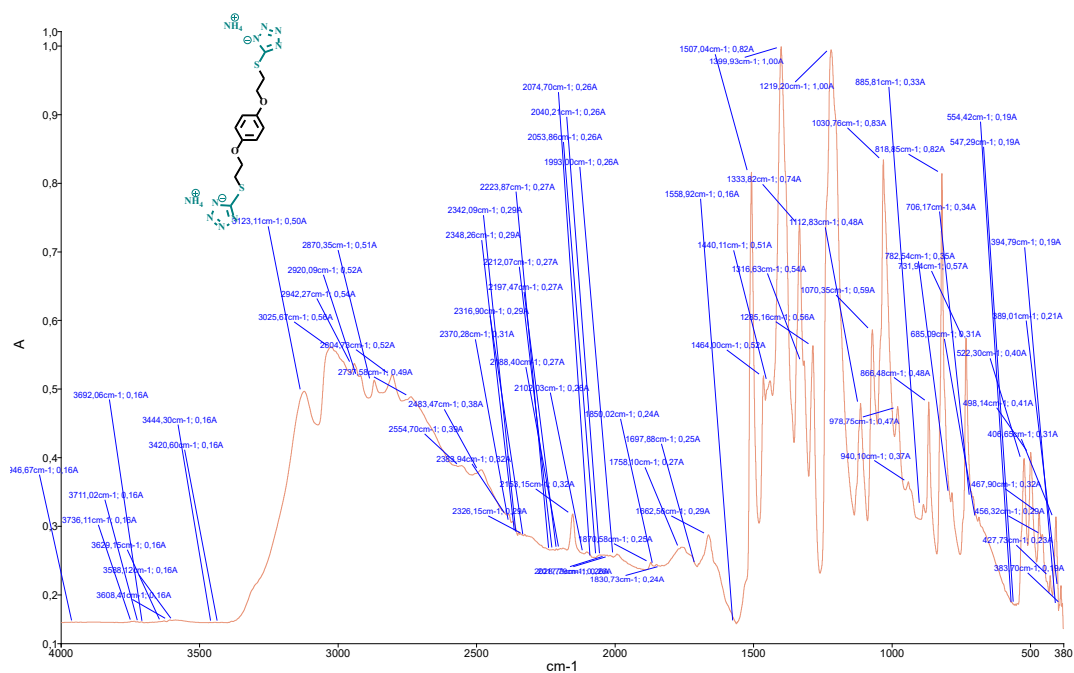


Figure S21. ^1H NMR spectrum of Ammonium salt of compound (**8**), D_2O , 298 K, 400 MHz.

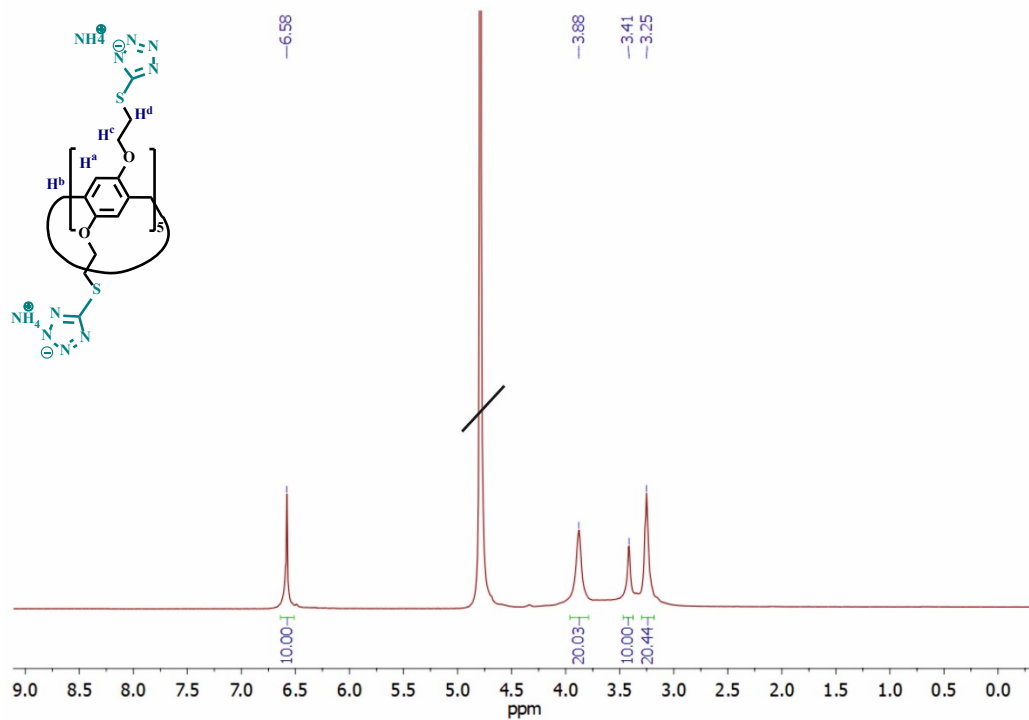


Figure S22. ^{13}C NMR spectrum of Ammonium salt of compound (**8**), D_2O , 298 K, 100 MHz.

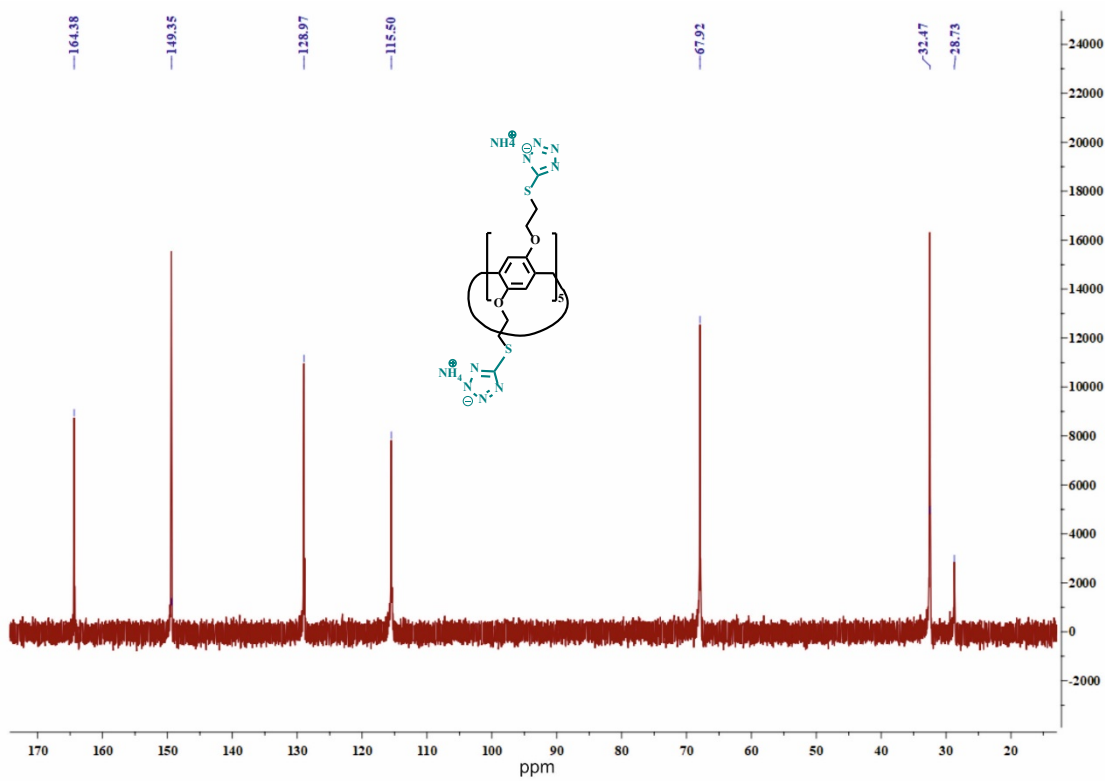


Figure S23. Mass spectrum (ESI) of Ammonium salt of compound (8).

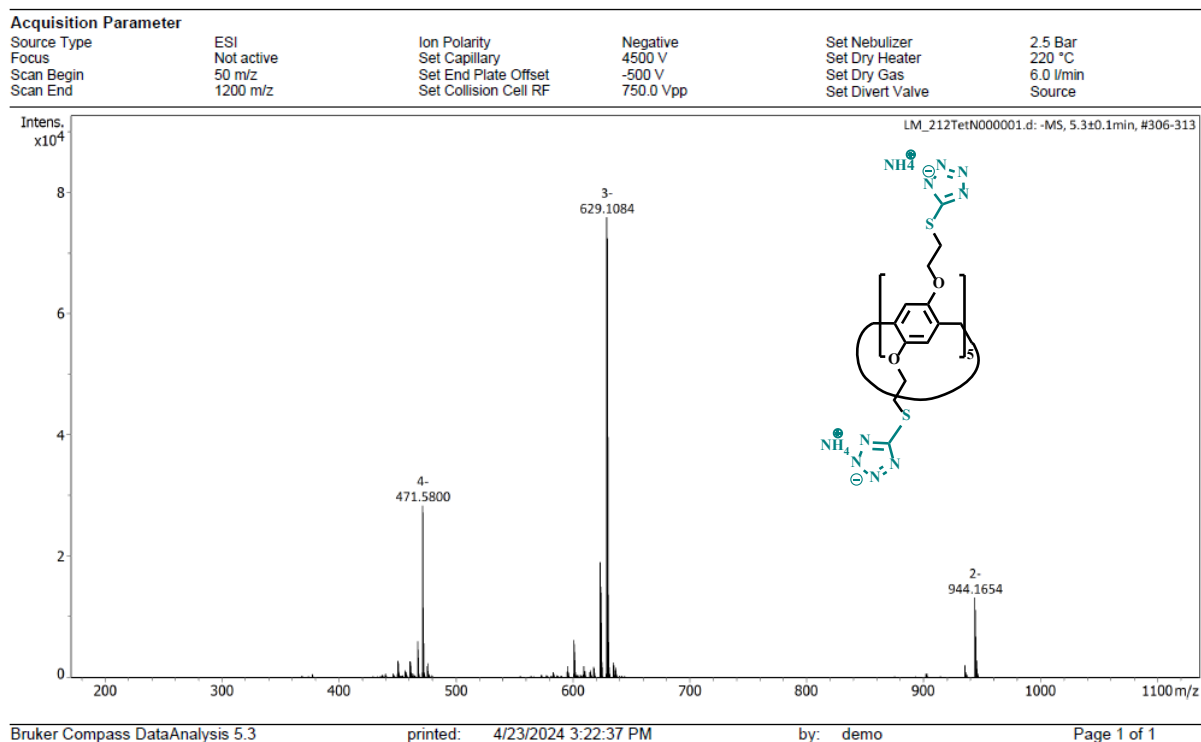
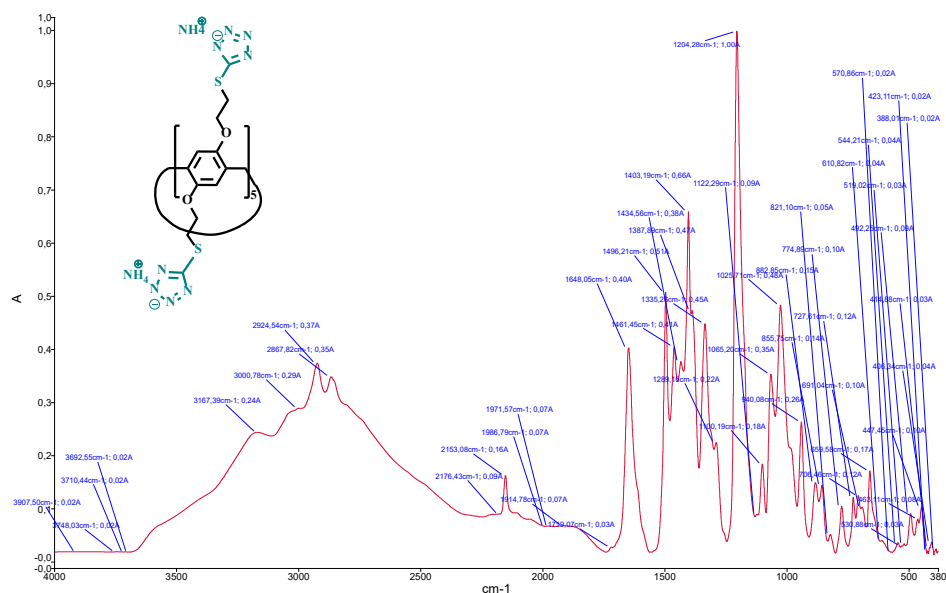


Figure S24. IR spectrum of Ammonium salt of compound (8).



2. Thermal Gravimetric Analysis of 3, 4 and 7, 8

Figure S25. TGA (green) and differential scanning calorimetry (DSC) (blue) curves of 3.

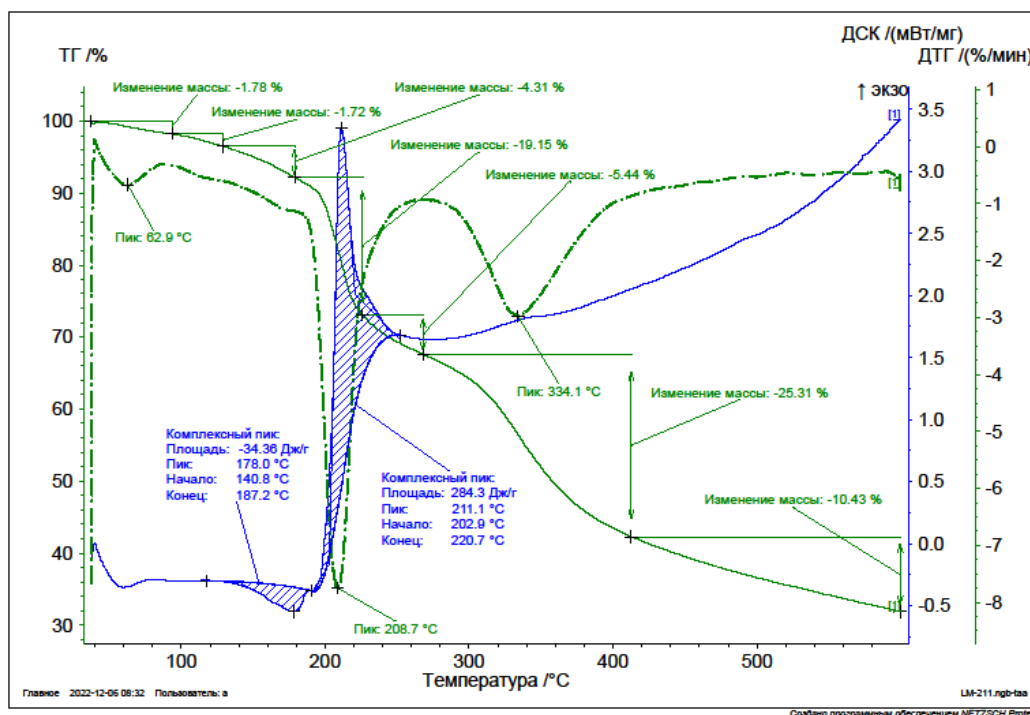


Figure S26. TGA (green) and differential scanning calorimetry (DSC) (blue) curves of 4.

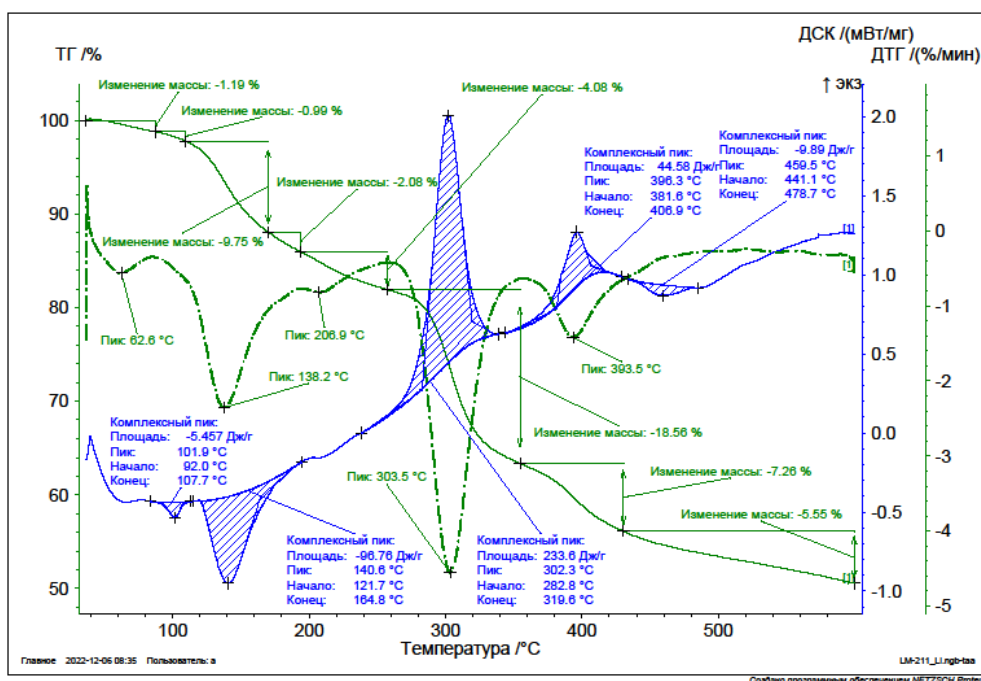


Figure S27. TGA (green) and differential scanning calorimetry (DSC) (blue) curves of 7.

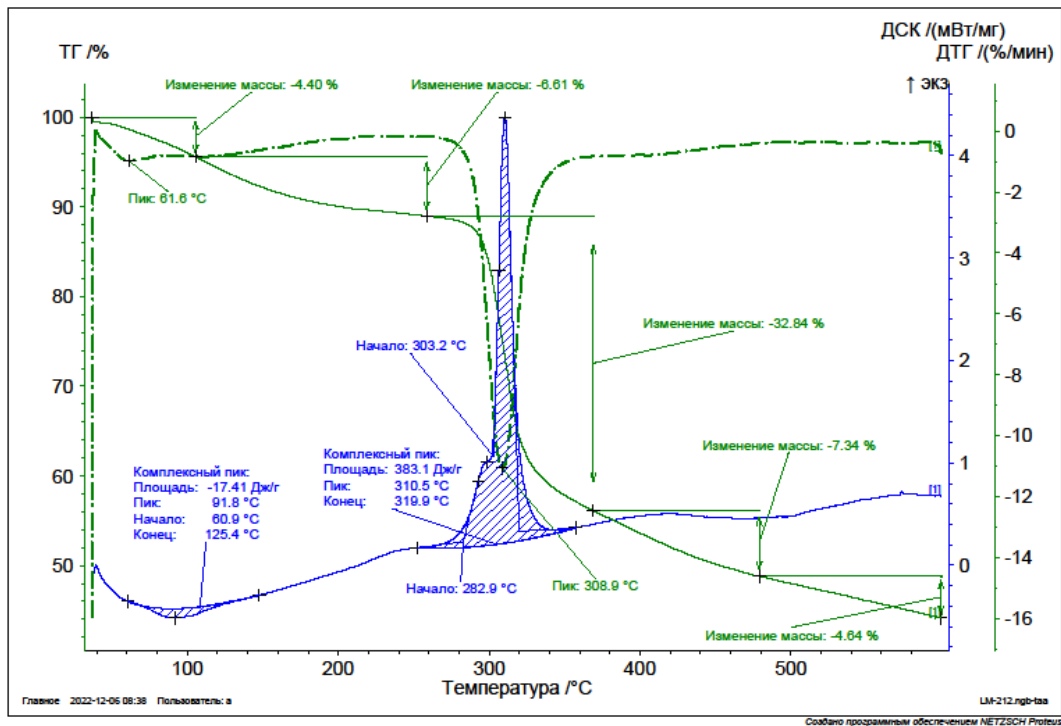
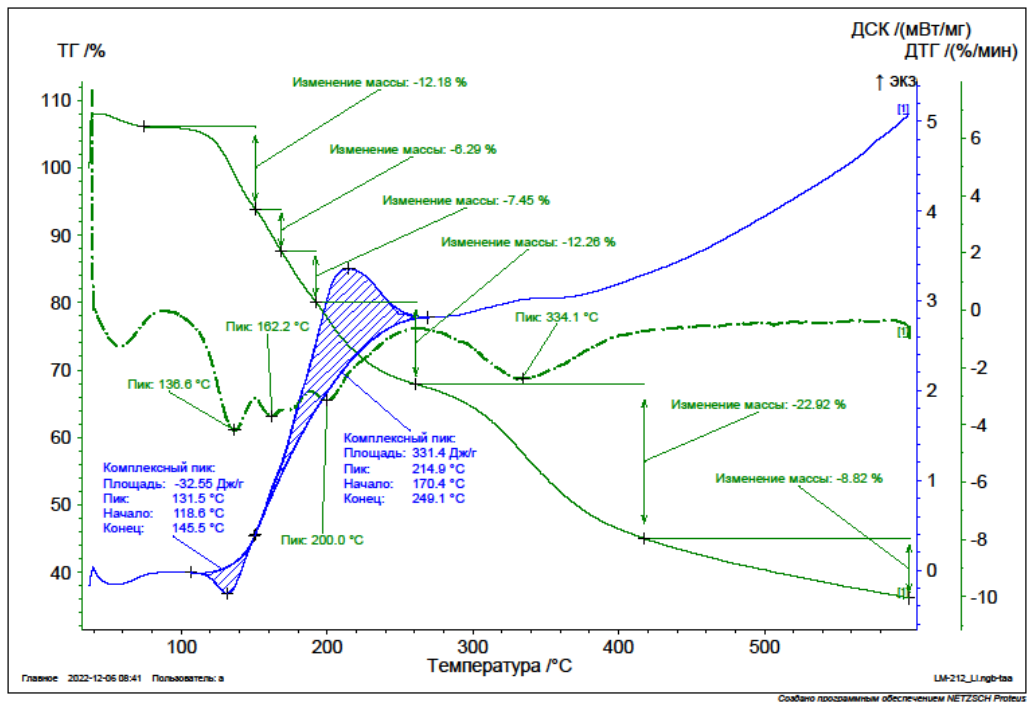


Figure S28. TGA (green) and differential scanning calorimetry (DSC) (blue) curves of 8.



3. UV spectra and Bindfit (Fit data to 1:1, 1:2 and 2:1 Host-Guest equilibria)

Figure S29. Bindfit (Fit data to 1:1, 1:2 and 2:1 Host-Guest equilibria) Screenshots taken from the summary window of the [website supramolecular.org](http://www.website-supramolecular.org). This screenshots shows the raw data for UV-vis titration of MB / **8** in water, the data fitted to 1:1 binding model (a), 1:2 binding model (b) and 2:1 binding model (c).

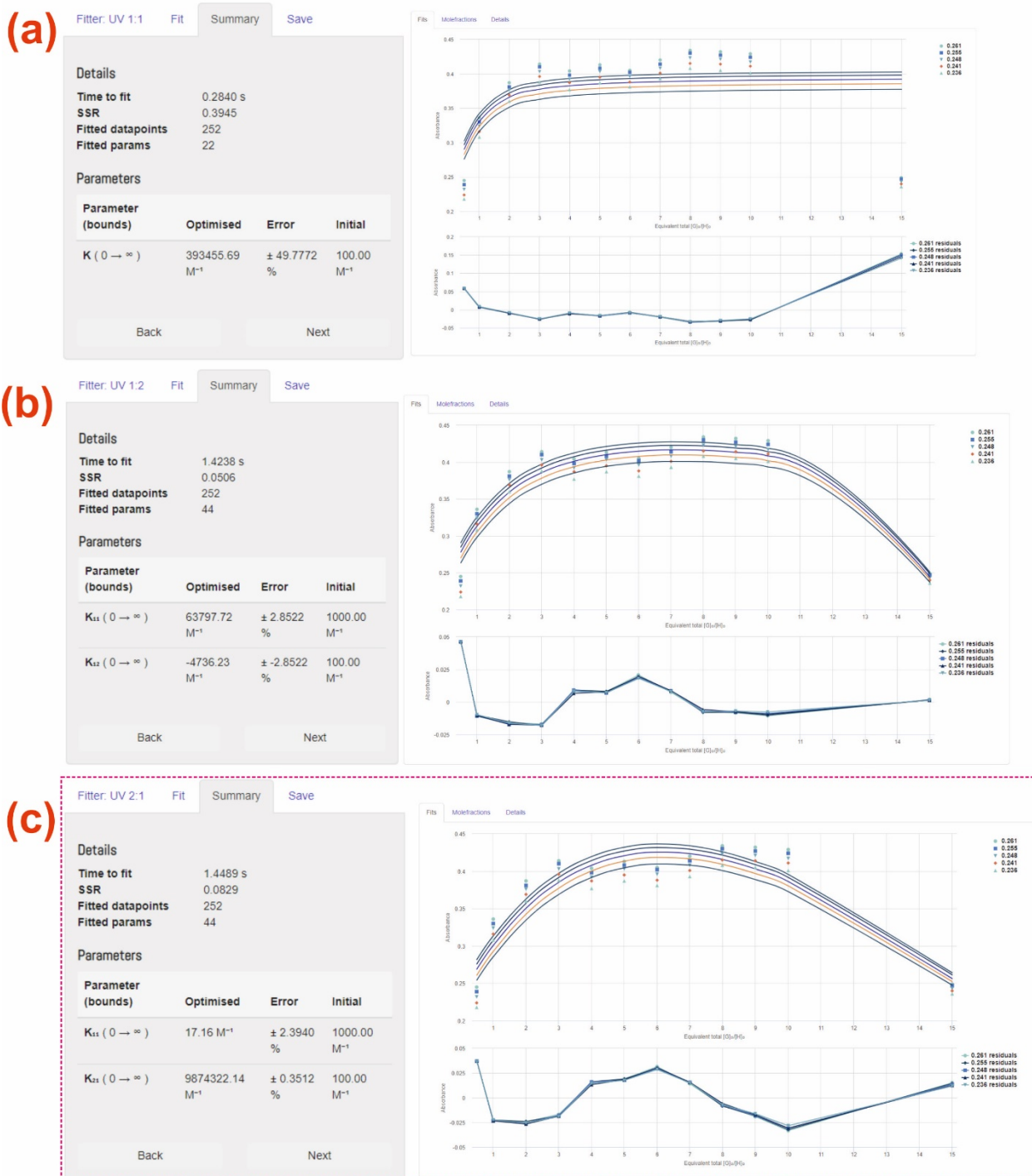


Figure S30. Bindfit (Fit data to 1:1, 1:2 and 2:1 Host-Guest equilibria) Screenshots taken from the summary window of the **website supramolecular.org**. This screenshots shows the raw data for UV-vis titration of MB / 7 in methanol, the data fitted to 1:1 binding model (a), 1:2 binding model (b) and 2:1 binding model (c).

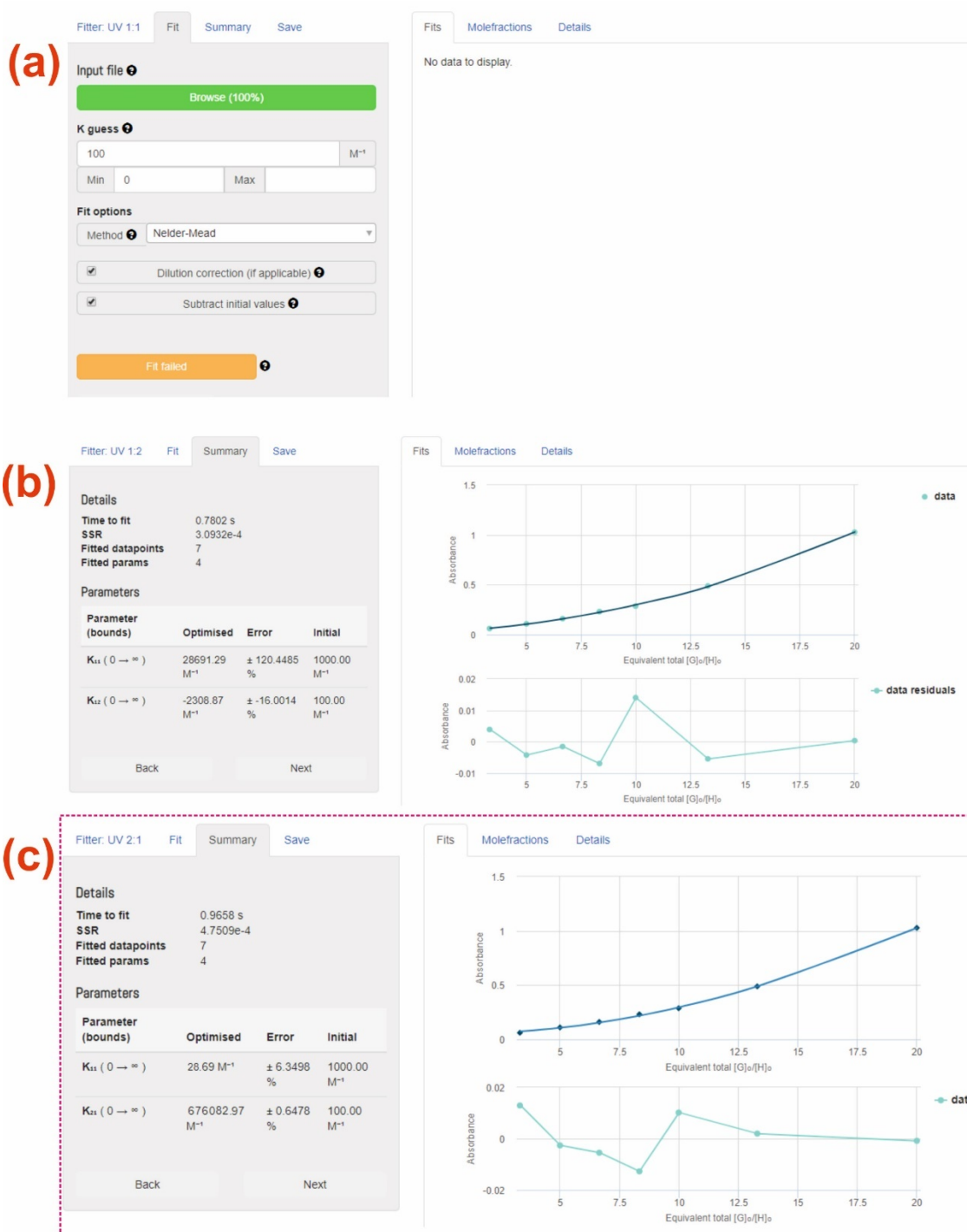


Figure S31. Bindfit (Fit data to 1:1, 1:2 and 2:1 Host-Guest equilibria) Screenshots taken from the summary window of the **website supramolecular.org**. This screenshots shows the raw data for UV-vis titration of $7 / \text{Zn}^{2+}$ in methanol, the data fitted to 1:1 binding model (a), 1:2 binding model (b) and 2:1 binding model (c).

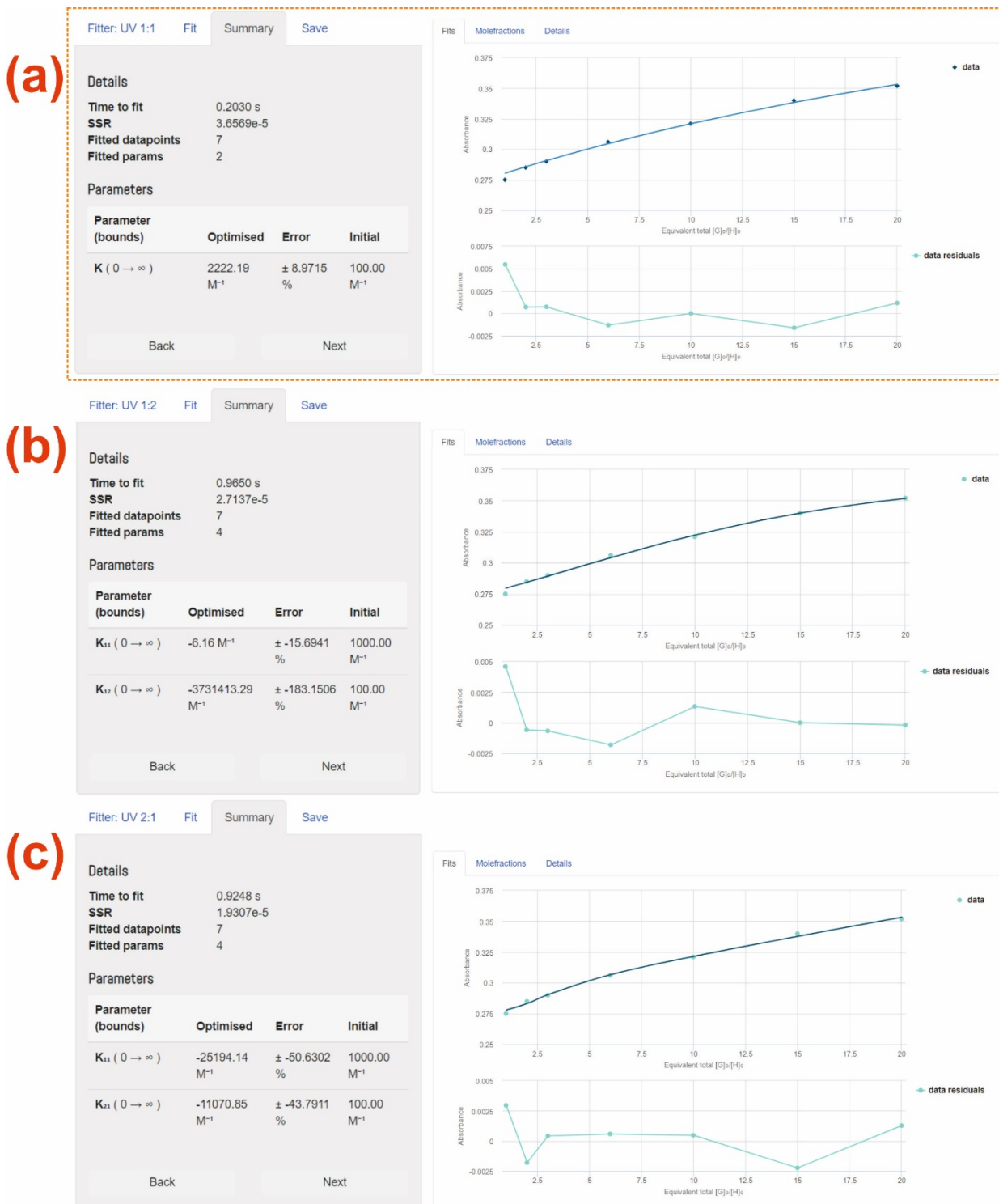


Figure S32. Bindfit (Fit data to 1:1, 1:2 and 2:1 Host-Guest equilibria) Screenshots taken from the summary window of the **website supramolecular.org**. This screenshots shows the raw data for UV-vis titration of $7 / \text{Co}^{2+}$ in methanol, the data fitted to 1:1 binding model (a), 1:2 binding model (b) and 2:1 binding model (c).

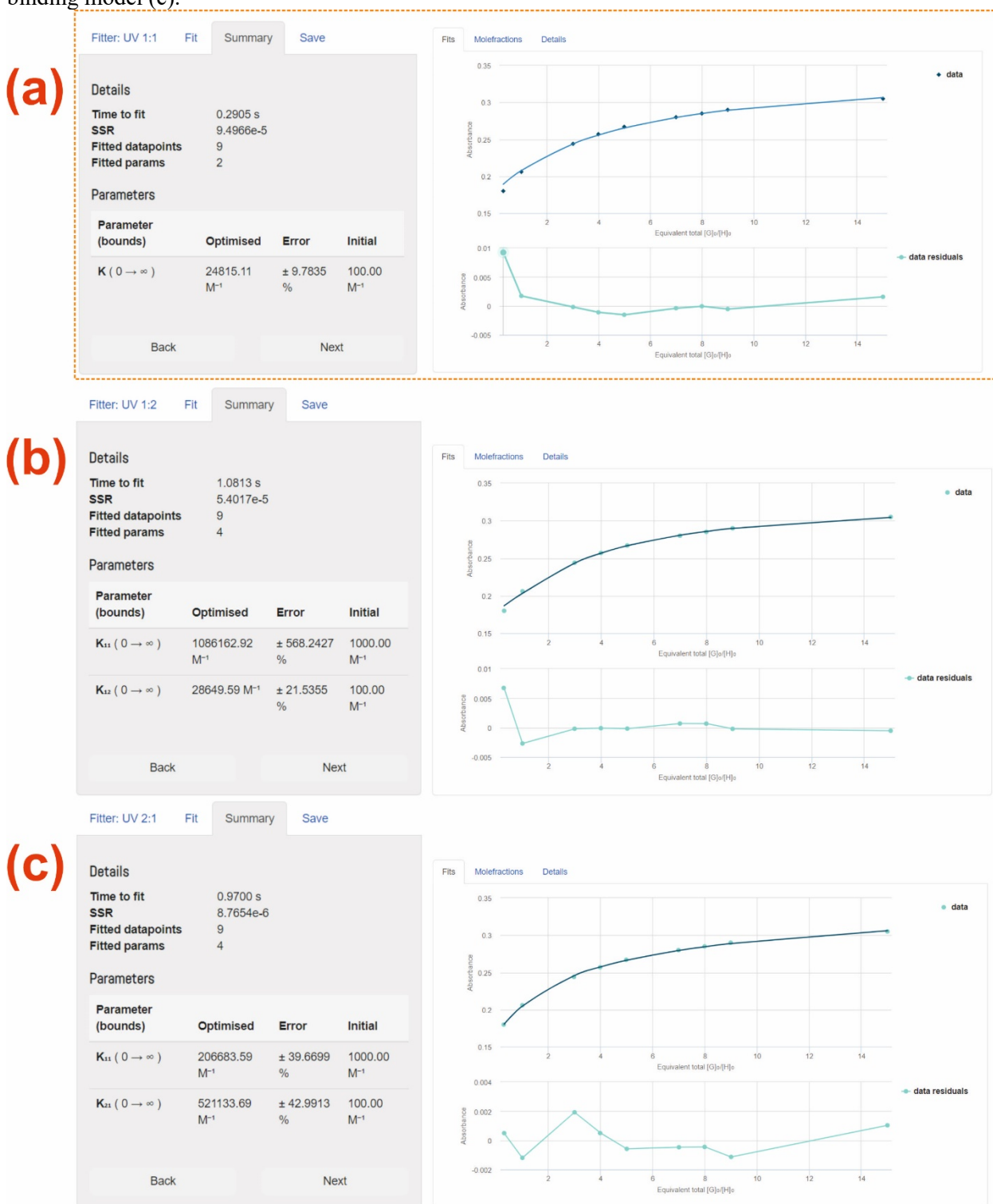


Figure S33. Bindfit (Fit data to 1:1, 1:2 and 2:1 Host-Guest equilibria) Screenshots taken from the summary window of the **website supramolecular.org**. This screenshots shows the raw data for fluorescence titration of **8** / Co^{2+} in water, the data fitted to 1:1 binding model (a), 1:2 binding model (b) and 2:1 binding model (c).

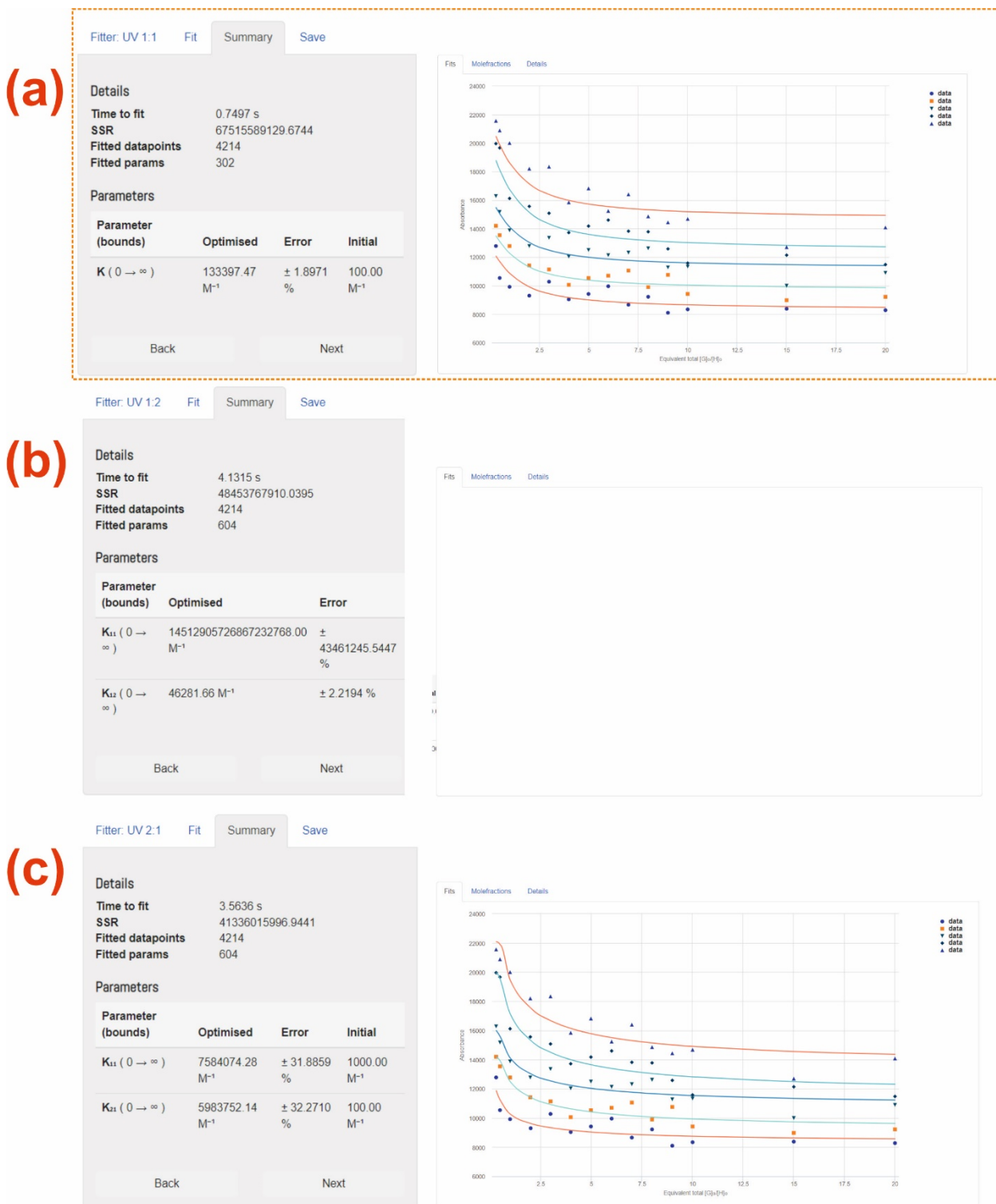
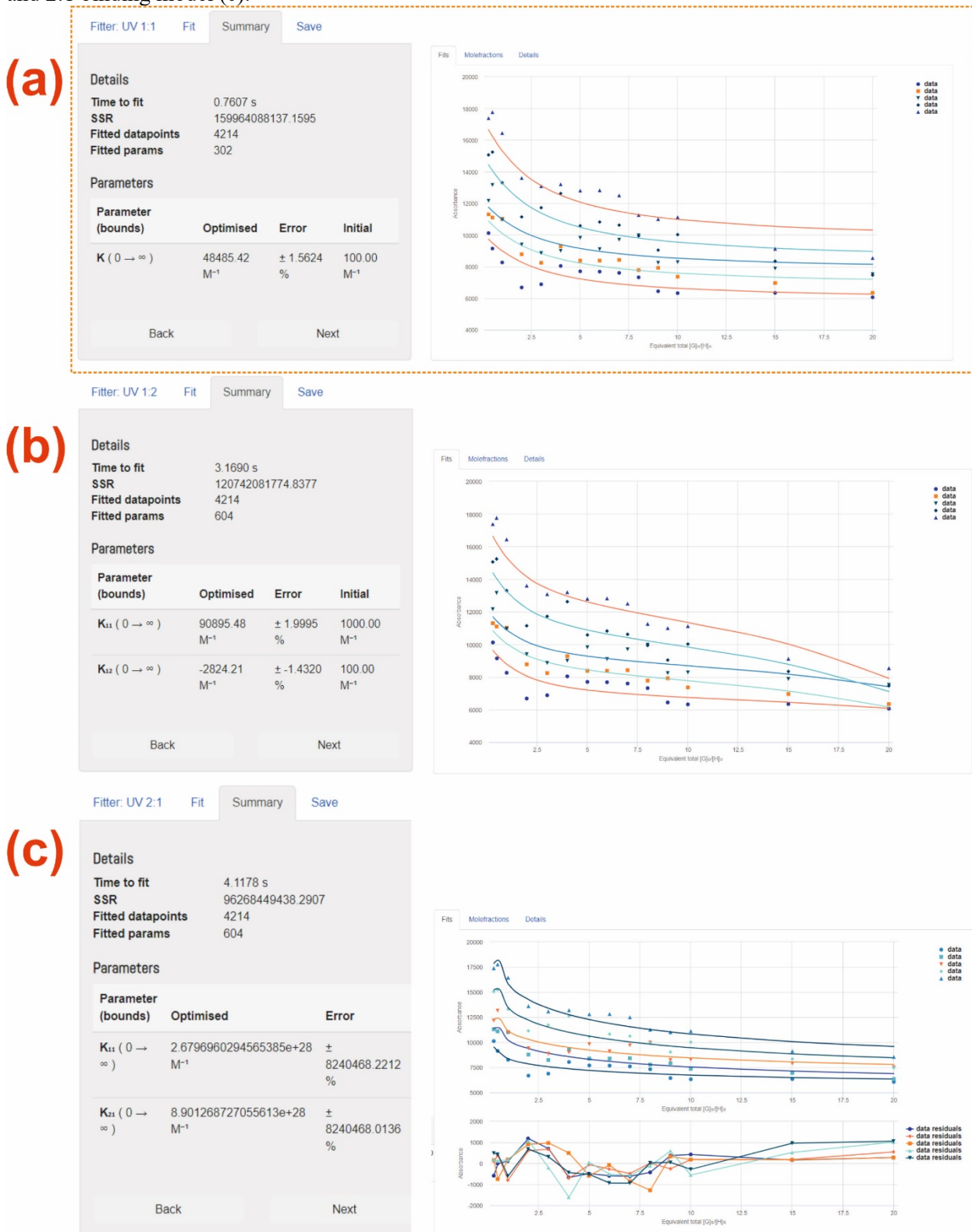


Figure S34. Bindfit (Fit data to 1:1, 1:2 and 2:1 Host-Guest equilibria) Screenshots taken from the summary window of the **website supramolecular.org**. This screenshots shows the raw data for fluorescence titration of **8** / Zn^{2+} in water, the data fitted to 1:1 binding model (a), 1:2 binding model (b) and 2:1 binding model (c).



4. Dynamic light scattering.

Table S1. DLS study on the aggregation for 7 with Zn²⁺ and Co²⁺ in the methanol

Ratio 7/Zn ²⁺	C ₇ , M (CH ₃ OH)	C _{Zn²⁺} , M (CH ₃ OH)	Z _{average} (d) , nm	PDI
1:0	1×10 ⁻³	0	1216±100	0.42±0.22
1:0	1×10 ⁻⁴	0	916±42	0.64±0.12
1:0	1×10 ⁻⁵	0	1015±131	0.54±0.11
1:1	1×10⁻³	1×10⁻³	981.6±10	0.22±0.09
1:1	1×10 ⁻⁴	1×10 ⁻⁴	842±32	0.39±0.12
1:1	1×10 ⁻⁵	1×10 ⁻⁵	798±25	0.44±0.20
1:2	1×10 ⁻³	2×10 ⁻³	-	0.9
1:2	1×10 ⁻⁴	2×10 ⁻⁴	531±15	0.32±0.09
1:2	1×10 ⁻⁵	2×10 ⁻⁵	512±32	0.49±0.19
2:1	2×10 ⁻³	1×10 ⁻³	1411±281	0.34±0.09
2:1	2×10 ⁻⁴	1×10 ⁻⁴	1215±171	0.51±0.21
2:1	2×10 ⁻⁵	1×10 ⁻⁵	1221±315	0.54±0.19
7/Co ²⁺	C ₇ , M	C _{Co²⁺} , M	Z _{average} (d) , nm	PDI
1:1	1×10⁻³	1×10⁻³	231±2	0.10±0.01
1:1	1×10 ⁻⁴	1×10 ⁻⁴	341±17	0.36±0.09
1:1	1×10 ⁻⁵	1×10 ⁻⁵	389±19	0.41±0.12
1:2	1×10 ⁻³	2×10 ⁻³	412±21	0.41±0.11
1:2	1×10 ⁻⁴	2×10 ⁻⁴	473±22	0.44±0.19
1:2	1×10 ⁻⁵	2×10 ⁻⁵	477±34	0.49±0.23
2:1	2×10 ⁻³	1×10 ⁻³	421±71	0.63±0.35
2:1	2×10 ⁻⁴	1×10 ⁻⁴	573±105	0.9
2:1	2×10 ⁻⁵	1×10 ⁻⁵	-	-

Table S2. DLS study on the aggregation for 7 / MB in MeOH.

Ratio 7/MB	C ₇ , M	C _{MB} , M	Z _{average} (d) , nm	PDI	ζ- potential, mV
1:0	1×10 ⁻⁵	0	388±66	0.31±0.01	
2:1	2×10 ⁻⁵	1×10 ⁻⁵	340±24	0.39±0.07	-
1:1	1×10 ⁻⁵	1×10 ⁻⁵	174±33	0.27±0.15	-
1:2	1×10 ⁻⁵	2×10 ⁻⁵	167±44	0.23±0.02	-
0:1	0	10 ⁻⁵	-	-	-
1:0	1×10 ⁻⁴	0	524±96	0.53±0.25	
2:1	2×10 ⁻⁴	1×10 ⁻⁴	226±34	0.42±0.13	
1:1	1×10 ⁻⁴	1×10 ⁻⁴	226±46	0.43±0.17	
1:2	1×10⁻⁴	2×10⁻⁴	142±5	0.21±0.04	18.42±0.04
0:1	0	1×10 ⁻⁴	-	-	-
1:0	1×10 ⁻³	0	216±18	0.62±0.23	
2:1	2×10 ⁻³	1×10 ⁻³	-	-	-
1:1	1×10 ⁻³	1×10 ⁻³	816±37	0.52±0.10	-
1:2	1×10 ⁻³	2×10 ⁻³	-	-	-
0:1	0	1×10 ⁻³	-	-	-

Table S3. Aggregation of the particles for **8** / MB in H₂O.

Ratio 8/MB	C ₈ , M	C _{MB} , M	Z average (d) , nm	PDI	ζ- potential, mV
1:0	1×10 ⁻⁵	0	87±3	0.39±0.05	
2:1	2×10 ⁻⁵	1×10 ⁻⁵	157.7±18.89	0.36±0.06	-
1:1	1×10 ⁻⁵	1×10 ⁻⁵	133.0±16.92	0.43±0.10	-
1:2	1×10 ⁻⁵	2×10 ⁻⁵	176.0±40.71	0.41±0.09	-
0:1	0	1×10 ⁻⁵	-	-	-
1:0	1×10 ⁻⁴	0	107±26	0.51±0.10	
2:1	2×10 ⁻⁴	1×10 ⁻⁴	98±3	0.42±0.06	-
1:1	1×10 ⁻⁴	1×10 ⁻⁴	80±14	0.41±0.07	-
1:2	1×10 ⁻⁴	2×10 ⁻⁴	72±1	0.30±0.03	21.10±0.03
0:1	0	1×10 ⁻⁴	-	-	-
1:0	1×10 ⁻³	0	87±2	0.38±0.04	
2:1	2×10 ⁻³	1×10 ⁻³	118±5	0.36±0.10	-
1:1	1×10 ⁻³	1×10 ⁻³	108±4	0.79±0.24	-
1:2	1×10 ⁻³	2×10 ⁻³	-	-	-
0:1	0	1×10 ⁻³	-	-	-

Figure S35. Size distribution of the particles by intensity for **8** (1×10⁻⁴ M) / MB (2×10⁻⁴ M) in H₂O

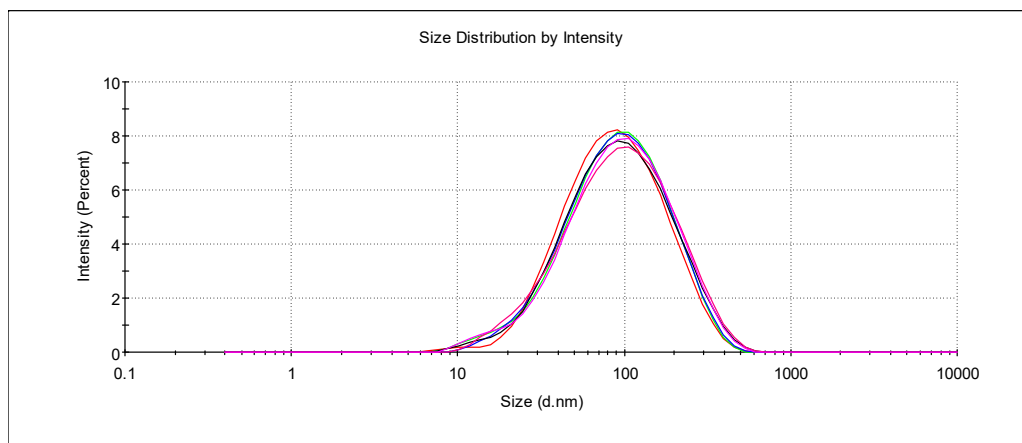
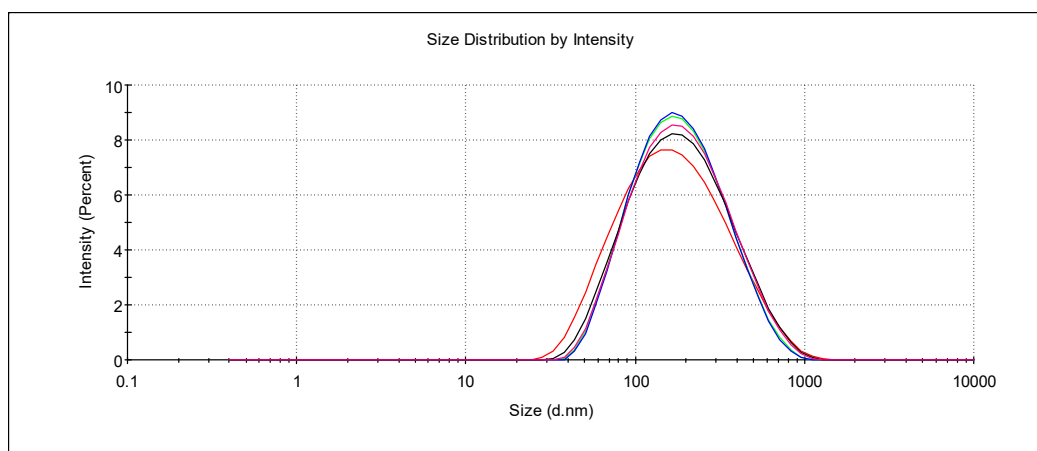


Figure S36. Size distribution of the particles by intensity for **7** (1×10⁻⁴ M) / MB (2×10⁻⁴ M) in MeOH



6. Electrochemistry

Figure S37. Cyclic voltammograms recorded on GCE in the solutions of MB (0.2 mM), compound 7 (0.1 mM) and metal salts (0.1 mM) at various pH

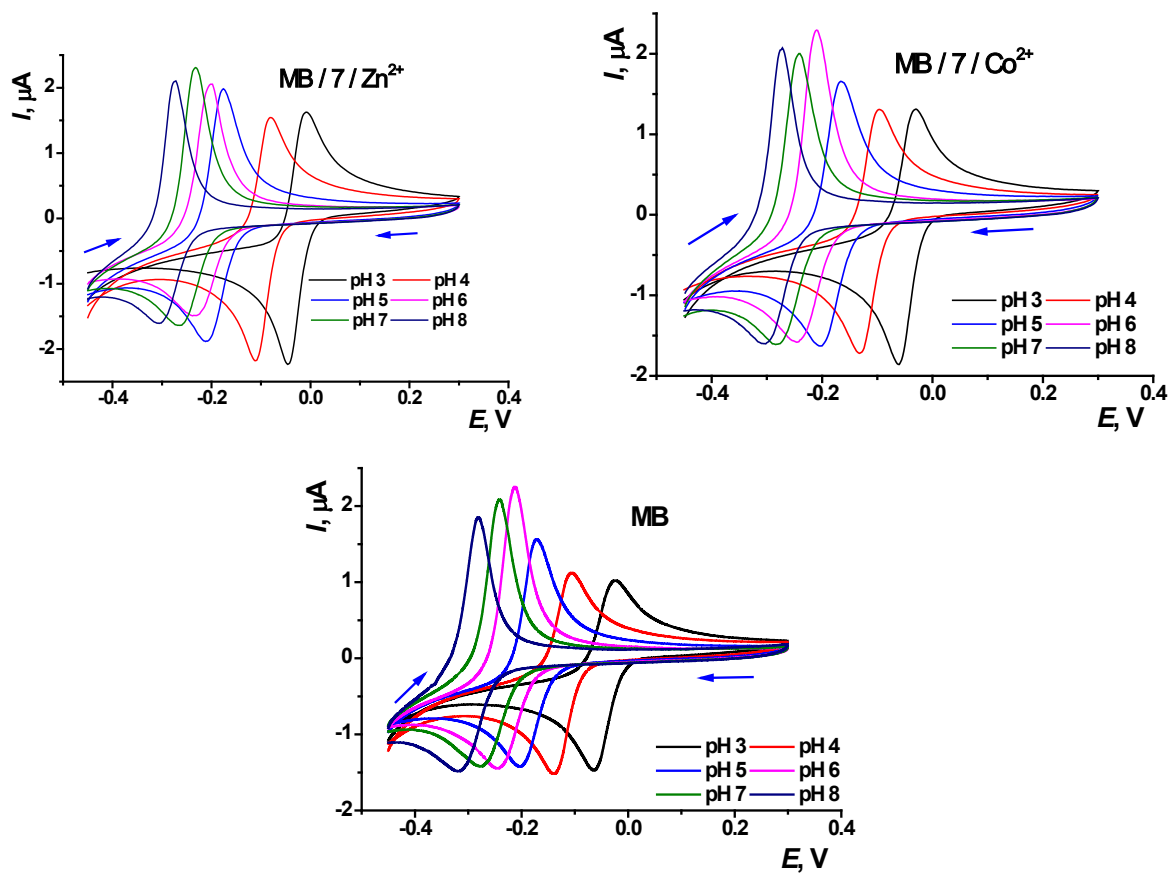
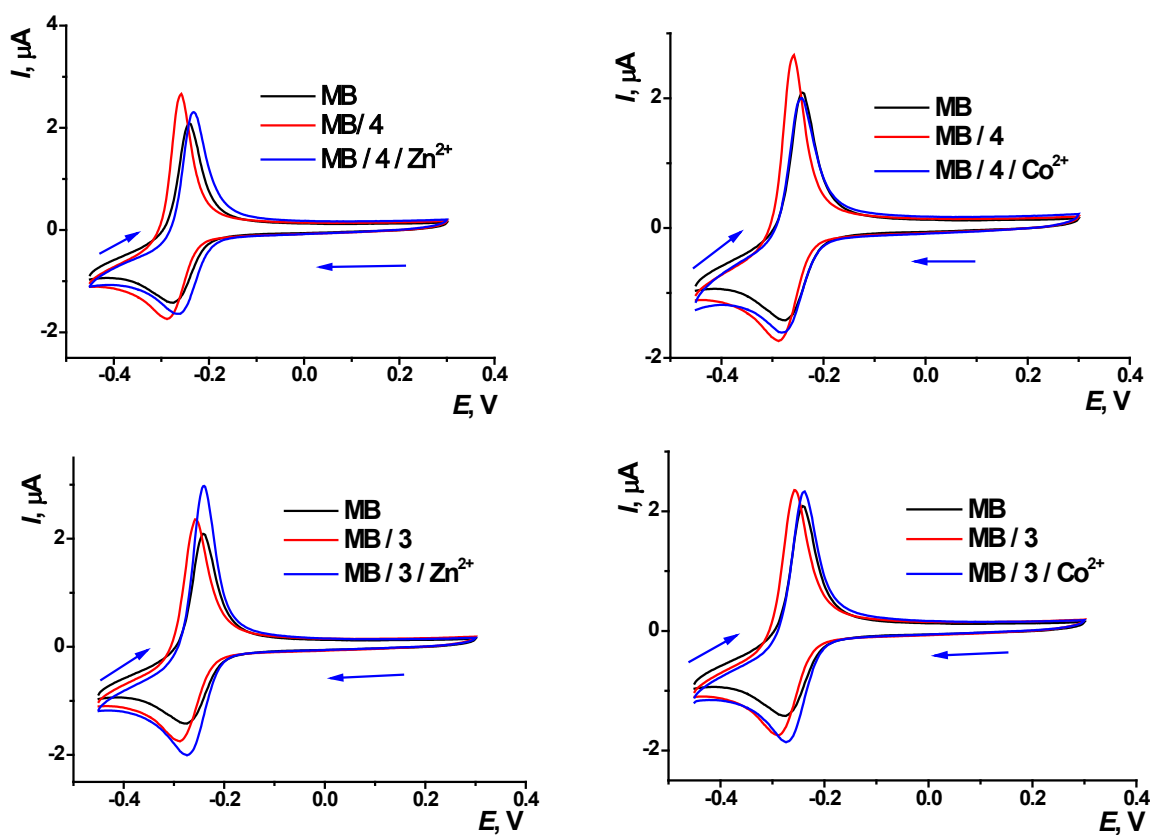


Figure S 38. Cyclic voltammograms recorded on GCE in the solutions of MB (0.2 mM), compounds **3** and **4** (0.1 mM) and metal salts (0.1 mM), HEPES buffer, pH 7.0, 50 mV/s.



7. Transmission electron microscopy

Figure S39. TEM images of self-associates **7** ($1 \times 10^{-4} \text{M}$)/MB ($2 \times 10^{-4} \text{M}$)

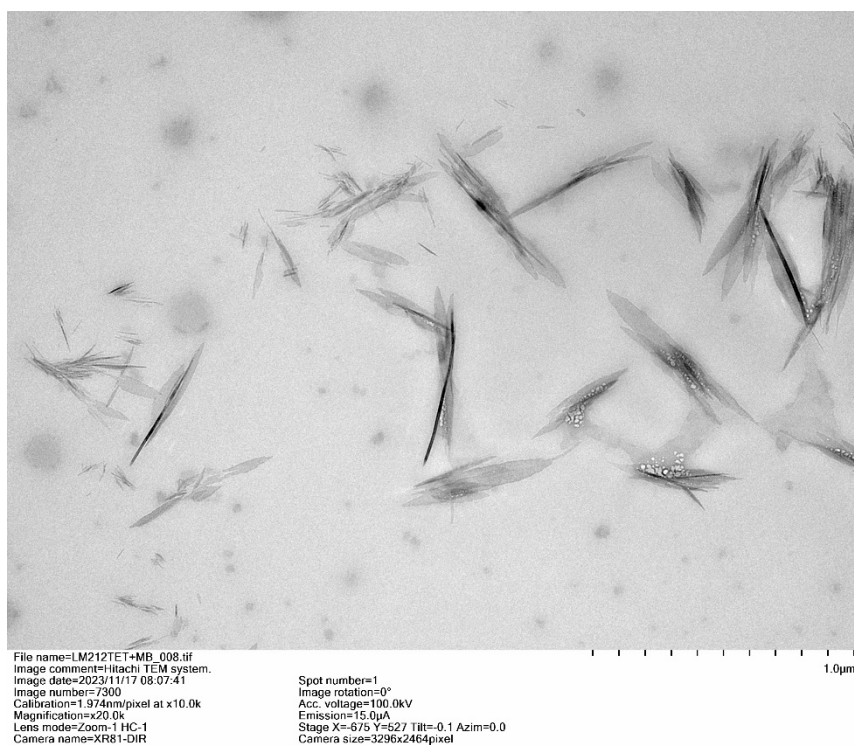


Figure S40. TEM images of self-associates **7** ($1 \times 10^{-4} \text{M}$)/MB ($2 \times 10^{-4} \text{M}$)

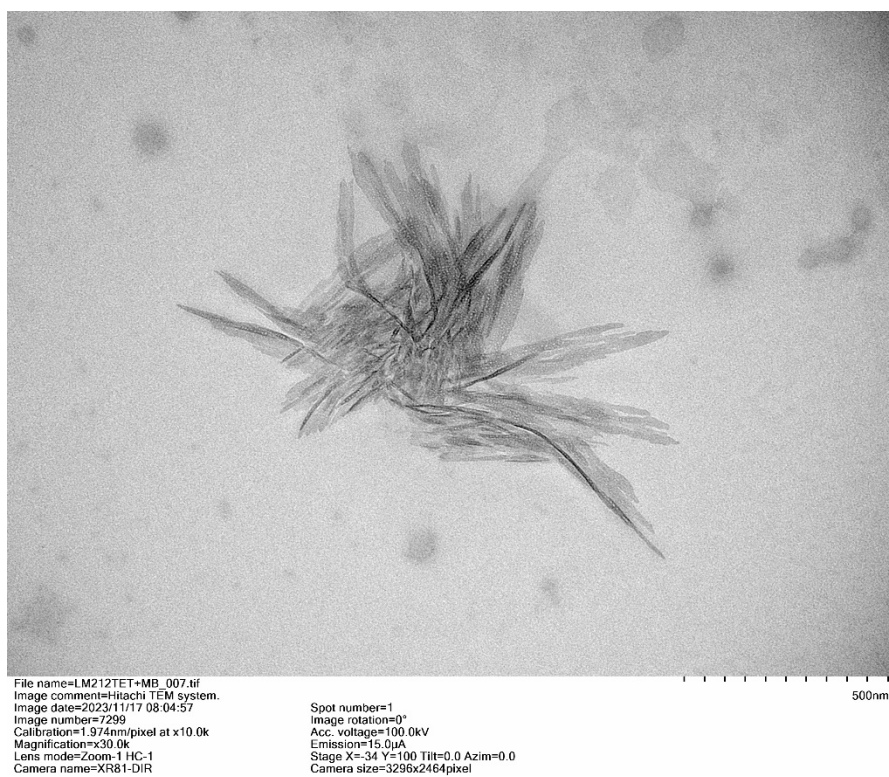


Figure S41. TEM images of self-associates **8** ($1 \times 10^{-4} \text{M}$)/MB ($2 \times 10^{-4} \text{M}$)

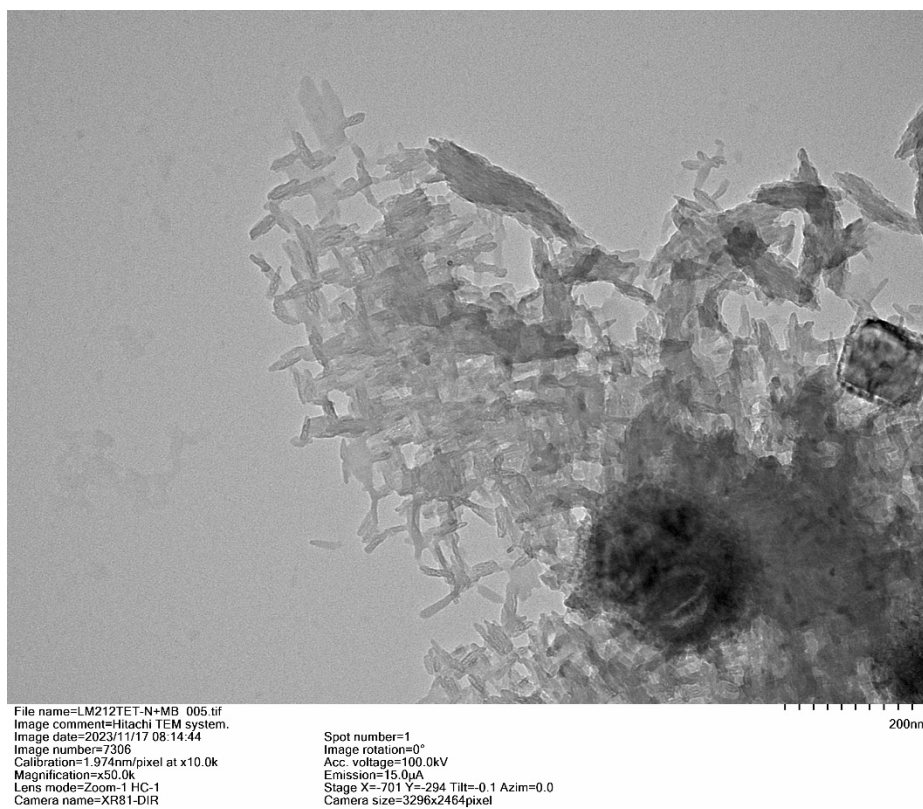


Figure S42. TEM images of self-associates **8** ($1 \times 10^{-4} \text{M}$)/MB ($2 \times 10^{-4} \text{M}$)

